Synthesis of studies on significant atmospheric electrical effects of major nuclear accidents in Chernobyl and Fukushima

Accepted version in: Science of the Total Environment, 733, 139271
https://doi.org/10.1016/j.scitotenv.2020.139271

Snežana Dragović[a*], Masatoshi Yamauchi[b], Michio Aoyama[c], Mizuo Kajino[d], Jelena Petrović[a], Mirjana Ćujić[a], Ranko Dragović[e], Milan Đorđević[e], József Bór[f]

Abstract

Radioactive materials released during the two most serious nuclear accidents in history, at Chernobyl and Fukushima, caused exceptionally significant contamination and perturbations of the environment. Among them, this paper focuses on the effects related to the atmospheric electricity (AE). Measurements of the most significant disturbances in the values of various AE parameters recorded near ground level are reviewed and the corresponding results are jointly evaluated. The Chernobyl and Fukushima events provided AE characteristics both after long-distance transport (Chernobyl) and short-distance transport including re-suspension (Fukushima). The data indicates that the electrical conductivity of the air is more sensitive to the presence of airborne radioactivity than the atmospheric electric potential gradient (PG). PG, on the other hand, can be monitored more easily and its variation also reflects the vertical redistribution of radionuclides in the air due to their transport, deposition, and re-suspension from the ground. A brief overview of studies on atmospheric transport and deposition of radioactive clouds is given to facilitate the importance of considering the AE measurements in these subjects, and of incorporating those studies in interpreting the results of AE measurements. The AE measurements is particularly important in studying microphysical effects of enhanced radioactivity in the air where no other distance monitoring method exists, both for fair weather conditions wet conditions.

Key words: radionuclides; transport models; atmospheric electric field; potential gradient

[a]University of Belgrade, Vinča Institute of Nuclear Sciences, POB 522, Belgrade, Serbia (correcpondence: sdragovic@vin.bg.ac.rs)
[b]Swedish Institute of Space Physics, Box 812, Kiruna, 98128, Sweden
[c]Center for Research in Isotopes and Environmental Dynamics, Tsukuba University 1-1-1 Tennodai, Tsukuba, Ibaraki 305-8572, Japan
[d]Meteorological Research Institute, Japan Meteorological Agency, 1-1 Nagamine, Tsukuba, Ibaraki 305-0052, Japan
[e]University of Niš, Faculty of Sciences and Mathematics, Department of Geography, POB 224, Niš, Serbia
[f]Research Centre for Astronomy and Earth Sciences, GGI, Hungarian Academy of Sciences, Sopron, Hungary

1. Introduction

Nuclear accidents in the Chernobyl Nuclear Power Plant in the Former Soviet Union and in the Fukushima Dai-ichi Nuclear Power Plant in Japan were serious disasters demanding many lives and causing severe damage to the environment. These events were rated at the maximum level (Level 7 - Major Accident) on the International Nuclear and Radiological Event Scale (INES). They caused outstanding disturbances and effects that do not occur normally, so that unambiguously associated response of different natural processes as well as that of the society could be surveyed. The two accidents are similar to each other in a sense that a large amount of radioactive material was injected into the atmosphere. Radionuclides spread and transported mainly by atmospheric circulation also caused severe contamination of the environment at great distances from the places of their origin. Having information on the expectable distribution and various effects of airborne radioactive material is of vital importance from the point of view of making right decisions for minimizing the associated damages. This study summarizes the results obtained from atmospheric electricity (AE) measurements in connection with these two major nuclear accidents.

Electrical processes in different regions of the Earth's atmosphere are interconnected and can be considered as elements of one complex system, referred to as the atmospheric global electric circuit (GEC) (Rycroft et al., 2012). The GEC is constantly powered by active thunderstorms and electrified shower clouds around the globe. Charged precipitation and convection currents transport naturally separated electric charges from these clouds to the ground and towards the lower ionosphere, creating a potential difference of 250-300 kV, i.e., an electric field between those two conductive spherical layers. The GEC is closed by low density vertical electric currents flowing over so-called fair weather areas which balance the ongoing charging of this planet-sized capacitor (Haldoupis et al., 2017). The state of GEC is most often characterized by near-surface measurements of the vertical direct current (DC) electric field, the inverse of which is called the atmospheric electric potential gradient (PG) (Nicoll et al., 2019). Direct measurements of electric conductivity, conduction current

density, and space charge density of the air contribute to a more complete local characterization of the GEC at different observation sites (Nicoll, 2012).

Under steady-state conditions, fair weather conduction current density does not depend on the altitude, therefore it is the vertical profile of the electric conductivity (e.g., Uman, 1986; Harrison and Bennett, 2007; Rycroft et al., 2008; Williams, 2009), which determines the vertical profile of the electric field (Ogawa and Morita, 1977; Bennett and Harrison, 2008). The electric conductivity is the smallest ($\sim 10^{-14}$ S m^{-1}) at the lowest 10 m - 1 km thick layer of the atmosphere, because the ionization rate is the smallest in that layer (Ogawa and Morita, 1977; Tuomi, 1988; Harrison and Bennett, 2007; Rycroft et al., 2008). At the lowest few to few tens of meters from the surface, the major ionization source is ionizing radiation due to the natural radioactivity of the solid Earth, e.g., due to radon gas. At greater altitudes, the ionization is determined mainly by cosmic rays. The flux intensity of cosmic rays, however, decreases exponentially with a rate of one order of magnitude within 15 km altitude difference as they penetrate deep inside the atmosphere from above (Ogawa and Morita, 1977).

As a result of low electrical conductivity, the electric potential gradient is the highest in the atmosphere near the ground. This property as well as the ease and relative simplicity of its measurement make PG a sensitive and cost-effective tool for monitoring any change in the lower atmosphere that is manifested in changes of the electric conductivity. For example, the variation of aerosol concentrations in an urban area is unambiguously mirrored by the variation of measured PG values (Harrison and Carslaw, 2003; Piper and Bennett, 2012; Jana and Maitra, 2019). Also, the daily variation of the ionized dust through convection (wind) under fair weather conditions is known to cause a corresponding variation in the measured PG values (Kondo, 1959; Harrison, 2003).

Radionuclides in the atmosphere increase the local conductivity by contributing to the ionization of the air. Increased local conductivity causes a drop in the PG. This effect was recognized first after nuclear tests in Tucson, Arizona, US (Harris, 1955). The PG measured near the ground dropped suddenly when a rain shower occurred, and this change was also accompanied by an increase of the ion density in the air at the same place. Low PG and the enhancement of the ion density continued for days after the rain was over. That near-surface effect can be attributed rather to the accumulation of the

93 radioactive material on the ground due to washout by precipitation than to radioactive
94 materials suspended in the air. Huzita (1966) discussed that the ionization rate from
95 airborne radioactive dust can be orders of magnitude lower than the ionization rate from
96 natural factors even over 1000 km away from emission source. Therefore, it is rather the
97 radioactive fallout accumulated on the ground which is responsible for the observed
98 change in PG. If the surface is contaminated by artificial radioactive materials, the
99 intensity of the ionizing radiation (beta and gamma rays) exceeds that from natural causes
100 (e.g., radon) by orders of magnitude. This results in a significant increase of electric
101 conductivity and a significant decrease of PG, as illustrated in Figure 1. This is the main
102 reason for radioactive fallout from nuclear tests in the 1950s and 1960s has been
103 diagnosed effectively by atmospheric electricity measurements (Pierce, 1972).

104 Pierce (1959) reported that about 100 km downwind the Windscale nuclear plant,
105 PG dropped statistically by >50% during 1952-1957. This was interpreted as a result of
106 accumulation of radioactive materials, which leaked from the nuclear plant, on the
107 ground. The accumulation may have happened via repeated events of dry deposition and
108 fixation to the soil by independent precipitation. It could also happened due to wet
109 deposition by relatively weak rains. Unfortunately, for Windscale case, no PG-drop
110 events at the arrivals of radioactive dust plumes and rain have been reported, and the
111 increased effect of wet deposition was taken into account only as an average factor.

112 These results also underline the importance of knowing the time evolution of the
113 state and properties of the radioactive contamination injected into the air from the point
114 of view of interpreting AE measurements correctly. The cloud of emitted fission products
115 quickly gets mixed with the air and, depending on the actual meteorological conditions,
116 can be transported far from the source. During atmospheric transport, the ionization
117 potential of the debris cloud is decreasing. This is due to dilution of the radioactive
118 material due to atmospheric mixing, radioactive decay of active isotopes in the plume,
119 and deposition processes (Crandall et al., 1973).

120 Deposition of radionuclides to the ground can be wet or dry (Panitz et al., 1989).
121 Wet deposition is the dominant process during precipitation (rain or snow), while dry
122 deposition is associated with sedimentation of aerosols. Soluble components may
123 undergo a longer atmospheric transport and can act as cloud condensation nuclei

(Lelieveld et al., 2012). Considering long distance, radioactive materials are transported by high-altitude (> few km) winds until they meet thick clouds with rain or snow which eventually causes them to fall out to the ground.

AE measurements, too, confirmed these long-distance scenarios. PG decreases due to nuclear tests were found to be significant world-wide, affecting even the smallest measured PG values near the ground during 1950s to 1960s (Pierce, 1959, 1972; Kondo, 1959; Hamilton and Paren, 1967; Harrison, 2003; Harrison and Ingram, 2005). In these observations, the radioactive fallout was caused by rain (wet deposition) after the world-wide transport in the stratosphere and upper troposphere.

In this work, we review the main results of AE-related research triggered by two of the most severe nuclear accidents inthe history. One aim of this work is to highlight the specific and unique contribution of AE measurements in assessing the impacts of nuclear accidents on the environment. This contribution contains new knowledge on atmospheric transport processes and effect of radionuclides on AE at the ground level. On the other hand, further investigations are suggested to exploit the results of these measurements mainly by incorporating them into complex studies on the atmospheric transport processes and on the recovering of the contaminated environment. Pullen et al. (2013) pointed out that both accidents revealed the need for improved analytical models for atmospheric but also water dispersion.

The timeline of the events and the properties of the corresponding radionuclides emitted into the atmosphere are briefly evoked in section 2. Main methods and the corresponding results of the investigations regarding the transport and the deposition of the radioactive material in the Earth's atmosphere are also summarized in this section. This is included with the intension to aid future research in which AE measurements may be used to support transportation models of airborne material. Additionally, characteristics of radionuclide transport may be considered more in the interpretation of AE measurements. Scientific research on AE-related effects of the two major nuclear accidents is reviewed in section 3. Note that this study focuses intentionally on results which are based on the most significant perturbations caused by the emitted radionuclides. This allows identifying the widest variety of related interactions among environmental parameters. Experiences found at separate measurement sites are jointly

evaluated and differences in principal research directions regarding the two cases happened 25 years apart are discussed in section 4. Finally, conclusions are summarized and suggestions regarding further research are given in section 5.

2. Timeline of the nuclear accidents and studies on the corresponding transport and deposition of radionuclides in the atmosphere

Radioactive material released to the atmosphere during the accidents can be carried by air masses over long distances before it gets deposited. The distance that radionuclides can travel before they are removed from the air depends on their physical and chemical properties and the weather conditions. In case of nuclear accidents, atmospheric dispersion models play significant role in predicting the movement of released radionuclides in the atmosphere and the deposition patterns of radioactive material all over the world. Comprehensive reviews of the models widely used for characterizing the distribution of radioactive pollutants on local, regional, and global scales are published by Leelőssy et al. (2018) and Bedwell et al. (2018). Uncertainties associated with these models are also addressed in these works. Utilization of atmospheric dispersion models in emergency planning and assessment of the propagation of the hazardous cloud following both Chernobyl and Fukushima accident are discussed by Benamrane et al. (2013).

2.1. The accident in Chernobyl

The accident at the Chernobyl nuclear power plant located in Ukraine about 20 km from its border with Belarus and 130 km north of Kyiv occurred on April 26, 1986 during the test of electric control systems at the graphite-moderated light water reactor. Operations conducted during the test led to a rapid increase of reactivity which further induced the vaporization of part of the fuel. The fuel steam expanded rapidly and, finally, caused an explosion which destroyed the largest part of the building. This resulted in the ejection of fuel, core components and some structural parts of the reactor to the

surrounding area (UNSCEAR, 2000). The emission of radioactivity from the damaged facility was prolonged by the fire of the graphite moderator which was burning for several days after the explosion. This accidental release caused contamination of both abiotic and biotic components of the environment as it was documented in many investigations following the accident (e.g. Sanada et al., 2002; Korobova et al., 2008; Dragović et al., 2010; Beresford et al., 2016).

In the first ten days after the Chernobyl accident, large amounts of radioactive material were released into the atmosphere with the total activities of about 14 EBq which included 1.8 EBq of ^{131}I, 85 PBq of ^{137}Cs and other cesium radioisotopes, 10 PBq of ^{90}Sr and 3 PBq of plutonium radioisotopes (IAEA, 2006). Physical and chemical forms of released material were presented in detail in the report of the International Atomic Energy Agency (IAEA, 2006).

The radioactive plume was transported across Europe and two days after the accident measurable radioactive signals were detected from an "unknown" source by automatic monitoring instruments in a Swedish nuclear power plant. Released radioactive materials were pushed into several directions by changing winds, which resulted in an uneven global distribution of radioactive materials and irregular deposited patterns over a wide area. Most affected countries were Belarus, the Russian Federation and Ukraine. A summary of the meteorological conditions (rainfall, changing wind direction) during the Chernobyl accident is given in Atlas map (see De Cort et al., 1998) and IAEA report (IAEA, 2006).

Hass et al. (1990) and Pudykiewicz (1988) used EURAD model and simplified version of the Eulerian LRTAP model, respectively, for simulation of the Chernobyl radioactive cloud. Based on chemistry transport model, Hass et al. (1990) show that near-surface part of the radioactive cloud spread out over most of the European countries until May 3, 1986. The model predicted that all other European countries except Ireland, Portugal and major parts of Spain were affected by dry deposition of ^{137}Cs, while Finland, the northern parts of Sweden and Norway, the Alpine region with north Italy and northern Yugoslavia, and the northern parts of Greece and downwind of Chernobyl were affected by wet deposition of ^{137}Cs (Hass et al., 1990). According to findings of Pudykiewicz (1988) the transport of radionuclides occurred in three stages: (1) from 25 to

the end of April - radionuclides were transported mostly over Europe, (2) from May 1-7 - radionuclides were transported from the Eastern to Western part of the Northern Hemisphere; and (3) after May 7 - radioactive cloud reached the East and West coasts of North America. Aircraft radioactivity measurements at 5000 m and 10000 m altitude above Europe, the Japan Sea and the West Coast of the United States indicated that accident-derived radioactivity has reached higher levels of the atmosphere than initially estimated.

A number of models have been used to assess the atmospheric dispersion of the Chernobyl plume such as MESOS, PATRIC and ADPIC (Ellis, 2003). The Lagrangian puff trajectory model MESOS has been developed with the purpose to simulate the atmospheric transport and dispersion of radionuclides across distances of several hundred kilometers and over (ApSimon et al., 1985). For assessing the period of release, MESOS follows the passage and dilution of a sequence of puffs released at intervals of 3 hours. Meteorological conditions along the paths of the puffs are also taken into account. One of the assumptions of the model is that materials released between these tracked puffs follow intermediate trajectories and dispersion. Daily variations in wind profiles, atmospheric stability, and mixing layer depth were merged over land and, separately, over the sea (ApSimon et al., 1987). Deposition behavior of material on the ground depends on the properties of the radionuclides. The PATRIC model was based on a three-dimensional puff and diffusion model, while the ADPIC model combined mass-consistent wind flow model and a particle-in-cell dispersion model (Ellis, 2003). Due to the rain, hotspots of wet deposition across Europe occurred. Unfortunately, in the mid-eighties of the last century it was impossible to model washout processes, because meteorological precipitation data or fine-scale forecast model precipitation products were not available at that time.

Talerko (2005a,b) used the model of atmospheric transport LEDI (Lagrangian-Eulerian Diffusion model) to reconstruct atmospheric transport and ground deposition of ^{137}Cs and ^{131}I, during the first 12 days after the Chernobyl accident, on the Ukrainian territory. A similar pattern was observed for ^{137}Cs and ^{131}I in air and ground contamination fields (Talerko, 2005b). According to Talerko (2005a), the deposition field in central Ukraine was formed predominantly due to dry deposition. Simulations of the

transport and deposition of the ^{137}Cs over Europe performed using the coupled model LMDZORINCA showed that ^{137}Cs was spread over very long distances affecting the most of the countries in Europe (Evangeliou et al., 2013b). A comprehensive study of reconstruction of the Chernobyl accident after 30 years was conducted by Evangeliou et al. (2016). Deposition maps of ^{137}Cs for Europe produced based on simulations of the Eulerian transport model LMDZORINCA (INCA) and the Lagrangian particle dispersion model FLEXPART were similar to the Atlas (De Cort et al., 1998). This confirmed the reliability of the models in predicting activity concentrations, cumulative deposition of ^{137}Cs and arrival times of the radioactive fallout (Evangeliou et al., 2016).

2.2. The accident in Fukushima

The Fukushima Dai-ichi nuclear power plant (FNPP) operated by the Tokyo Electric Power Company (TEPCO) is located in Fukushima Prefecture of the Tohoku region in Japan about 230 km northeast of Tokyo. On March 11, 2011 the earthquake of magnitude 9.0, the largest ever recorded in Japan, occurred as a result of extensive fault ruptures on or near the boundary between the Pacific and North American tectonic plates. The earthquake with a hypocenter depth of 24 km occurred around 130 km offshore the city of Sendai. Immediately after the earthquake, the FNPP reactors were switched off and the fission process was stopped. However, subsequent tsunamis of more than ten meters high inundated the FNPP facilities and disabled the operation of generators for reactor cooling pumps. This led to the melting of nuclear fuel, a series of hydrogen-initiated explosions and severe damage of the cores of three reactors (UNSCEAR, 2013; IAEA, 2015).

A large amount of radioactive material was released into the atmosphere from the three damaged cores. Emitted isotopes dispersed across the entire globe in the directions of the prevailing winds (Lin et al., 2015; Thakur et al., 2013) (Figure 2). Meteorological conditions (rainfall, changing wind direction, pressure) during the Fukushima accident are overviewed by the WMO (2013). About two weeks after the accident, radionuclides from Fukushima were detectable across the entire Northern Hemisphere. By April 13,

radioactive materials eventually also reached the southern hemisphere in the Asia-Pacific region (CTBTO, 2011).

More than 99% of the radioactivity released into the air after Fukushima accident was due to highly volatile radionuclides such as I, Te, Cs, Xe, and Kr (Mathieu et al., 2018). The total released amounts of the top major radionuclides are estimated as ^{133}Xe (6 - 20 EBq), ^{131}I (100 - 400 PBq), ^{132}Te-^{132}I (87.1 PBq; (Katata et al., 2015)), ^{134}Cs (10 - 35 PBq) and ^{137}Cs (15 - 21 PBq) (Aoyama et al., 2020). The physical half-lives of ^{133}Xe, ^{131}I, ^{132}Te-^{132}I, ^{134}Cs, and ^{137}Cs are 5.25 d, 8.0 d, 3.2 d-2.3 h, 2.1 y, and 30.0 y, respectively. Chemical and transportation characteristics of fission products from the Fukushima accident were presented in detail in the review paper of Koo et al. (2014).

Numerical simulations were commonly used for source term (i.e., quantity of radionuclides released in the atmosphere) estimation following the Fukushima accident. Chino et al. (2011) used an inverse estimation of the source term of iodine and cesium discharged from the FNPP into the atmosphere in the first days after the accident. The method applied was based on the coupling of environmental monitoring data with atmospheric dispersion simulations under the assumption of unit release rate (1 Bq h^{-1}).Several source term assessments have been conducted following the accident using environmental data at both local (Katata et al., 2012; Korsakissok et al., 2013) and large scale (Stohl et al., 2012; Terada et al., 2012; Winiarek et al., 2012).

The behavior of the most important radionuclides released after the Fukushima accident has been extensively studied through atmospheric dispersion modelling and model intercomparison studies (e.g., Morino et al., 2011; Stohl et al., 2012; Evangeliou et al., 2013a; Marzo, 2014; SCJ, 2014; Draxler et al., 2015; Katata et al., 2015; Nakajima et al., 2017; Sato et al., 2018). Atmospheric dispersions of radionuclides were simulated by successive uses of the meteorological prediction model PHYSIC and the atmospheric dispersion models PRWDA21 in SPEEDI, and MM5 and GEARN in WSPEEDI-II (Nagai et al., 1999; MEXT, 2007; Terada et al., 2008a,b). Morino et al. (2011) applied a three-dimensional chemical transport model, Models-3 Community Multiscale Air Quality (CMAQ) in order to simulate the distributions of radioactive isotopes ^{131}I and ^{137}Cs at a regional scale during March11-30, 2011. The model roughly reproduced the observed spatiotemporal variations of deposition rates over 15 prefectures in Japan, some

discrepancies between the simulated and observed data can be attributed to model uncertainties (Morino et al., 2011).

Stohl et al. (2012) estimated that 18% of the total ^{137}Cs deposition until April 20 (i.e., 6.4 PBq) occurred over land in Japan. Evangeliou et al. (2013a) used the atmospheric transport model LMDZORINCA to simulate the global transport and deposition of the ^{137}Cs after the Fukushima accident. For the analysis of the atmospheric flows of the ^{137}Cs, Nakajima et al. (2017) used a combination analysis of two aerosol transport models and hourly observed ^{137}Cs concentrations at surface level during March 14-23, 2011. The model ensembles revealed the main features of the atmospheric ^{137}Cs distributions and transport routes of eight ^{137}Cs plumes during the studied period. However, some differences between the observed and simulated results were found indicating the need for model improvements (Nakajima et al., 2017).

Model inter-comparison (or sensitivity) studies (e.g., Adachi et al., 2013; Morino et al., 2013; Katata et al., 2015; Quérel et al., 2015) can be used to identify the sources of ambiguity in the models. Such studies have been conducted regarding the dispersion and deposition of radionuclides in Japan not only for the sake of simple comparison but also for investigations on transport and deposition mechanisms. The major conclusions obtained from the different inter-comparison studies are coherent. Key points are summarized as follows: (1) there are still significant uncertainties in deposition modeling; (2) it is hard to determine the best model in all aspects, but the ensemble mean can be reasonable in all aspects, and (3) most model inter-comparison studies compare different models with unique or different inputs. The inter-comparison made by Kajino et al. (2019) was different from these in a sense that they compared the output of one model fed with different inputs, i.e., nine different meteorological simulations with a given source term and transport model. This proved to be a useful strategy for evaluating the performance of the applied transport model.

Approximately 80% of the radioactive material that was released from FNPP, including what was emitted into the atmosphere, was eventually deposited into the ocean. This enabled a unique approach in this case in which radionuclide measurements in water are used to complete the knowledge on atmospheric circulation and on the matter exchange between the atmosphere and the ocean. East of the coast of the largest Japanese

island Honshu is the collision zone of the warm Kuroshio and the cold Oyashio marine currents, which interacted with the air circulation and indirectly influenced the dispersion of radioactive particles and gases into the atmosphere. The behavior of FNPP-released radioactivity in the marine environment are summarized by Aoyama et al. (2016a,b) and Buesseler et al. (2017).

North Pacific inventory of ^{137}Cs, calculated from samples from the surface above a standard mixed layer of 50 m over 10 degree x 10 degree areas between 20°N - 50°N, was estimated to be 15-18 PBq (Aoyama et al., 2016a). This result is in accordance with estimates obtained from more comprehensive ocean data sets and by interpolation methods and models - 15 PBq by Inomata et al (2016), and 16 PBq by Tsubono et al. (2016). Close to the FNPP site, direct discharge was the dominant process to form the radioactivity distribution pattern. Inomata et al. (2014) found strong correlations between *in-situ* activities of ^{131}I, ^{134}Cs, and ^{137}Cs measured in surface seawater samples and gamma-ray peak count rates determined by the aerial survey (correlation coefficients were 0.89 for ^{131}I, 0.96 for ^{134}Cs, and 0.92 for ^{137}Cs).

The offshore area of high radionuclide activity extended south and southeast from the FNPP. The ^{131}I/^{137}Cs ratio in surface water of the high-activity area ranged from 0.6 to 0.7. Considering the radioactive decay of ^{131}I, they determined that the radionuclides in this area were directly released from FNPP to the ocean. Following the accident, both ^{134}Cs and ^{137}Cs are observed in a wide area in the North Pacific Ocean (Aoyama et al., 2013). The horizontal distribution of ^{134}Cs of FNPP-origin in the western North Pacific Ocean except just in front of the FNPP site showed that the high concentration area was located close to the FNPP accident site. In addition to direct discharge from the FNPP site (Tsunume et al., 2012), deposition from the atmosphere might also have contributed to the increased level of radioactive contamination in this area. This scenario is consistent with the atmospheric transport model study of Honda et al. (2012).

Povinec et al. (2013) predicted that radionuclides released in Fukushima accident will reach the west coast of the United States in about five years. The FNPP-derived ^{134}Cs has found to be spread and was first observed at the westernmost station on Line P, an oceanographic sampling line extending 1500 km westward of British Columbia (BC), Canada in June 2012 (Smith et al., 2017). Highly contaminated water reached west coast

of North American continent in 2015 (Smith et al., 2017; Kumamoto et al., 2019). Ocean circulation model simulations that are consistent with the time series measurements of Fukushima ^{137}Cs indicate that the 2015–2016 results represent maximum tracer levels (Tsubono et al., 2016). It was also detected in two water samples from the Bering Sea (Kumamoto et al., 2016, 2017). The increase in the Bering Sea was probably derived from the long-range transport of the FNPP1-derived radiocesium into the Bering Sea with the subarctic gyre circulation in the North Pacific (Kumamoto et al., 2019). Huang et al. (2020) reported the presence of FPNN-derived ^{134}Cs and ^{137}Cs in subarctic regions and the Arctic Ocean (Chukchi Sea) in 2017 and attributing it to their transport from the Pacific Ocean into the Bering and Chukchi Seas by ocean currents. They also hypothesized that these radionuclides will be continuously transported into the Canada Basin and Arctic Ocean through the Bering Strait in the next several years.

3. Direct and indirect effects of radionuclides from the accidents on near-surface AE measurements

3.1. Atmospheric electrical effects of the Chernobyl accident

The propagation and extension of the radioactive plume over Europe was confirmed by atmospheric electricity measurements at several measurement sites across the continent.

3.1.1. Measurements in Swider, Poland

The rich set of measurements in Swider, Poland provided a unique opportunity for the complex analysis of environmental changes related to the event. Recordings of PG were completed by measurements of atmospheric conductivity (for both positive and negative ions), radioactive fallout (Bq m^{-2}, on a weekly cycle), aerosols, i.e., the concentration of condensation nuclei, and meteorological parameters (rain accumulation, wind, and cloudiness). A detailed report on the observations in 1986 was published by Warzecha (1987). Later, the author discussed the extension of the analysis up to 1987

(Warzecha, 1991). The arrival of the radioactive contamination at Swider was detected already on the next day of the accident by the simultaneous increase in air conductivity and decrease in PG. The conductivity increased most dramatically in the next couple of days to about ten times the average value before the accident. The lowering of the PG to about 30% of the undisturbed average was less explicit; nevertheless the anti-correlation with the changes in the conductivity was unambiguous. Note that all these changes accompanied an over 100-fold increase in the radioactive fallout density.

Several features of the observations were noted. (1) When the ionization intensity was at the peak, the conductivity from negative ions was larger than that from the positive ions. Note that positive conductivity typically exceeds the negative one because negative ions get more easily attached to low mobility large particles (Kawano et al., 1969). (2) High daytime conductivities persisting for several days decreased considerably during nights. It was suggested that this was due to the cutoff of downward transport of radioactive nuclei from higher altitudes because of the stabilization of the boundary layer during nights. (3) Despite the increased level of ionization, the concentration of condensation nuclei near the surface did not grow but it was rather decreased. It was hypothesized that the produced ions were too small to be detected as aerosols. Note that the 1.5 weeks long period following the accident discussed in detail in the report by Warzecha (1987) could be considered as fair weather with practically no precipitation, only few clouds and low wind speeds (Harrison and Nicoll, 2018). In this sense, observation at Swider marks the first-time detection of dry deposition event (Warzecha, 1987, 1991).

The activity concentration of radioactive fallout peaked in May 1986 and it remained relatively high in the rest of the year. In December 1986, it was still ten times higher than the value before the accident. The anomalously high radioactivity concentration remained for a whole year until only after May, 1987. Measurements of the deposition showed that radioactive substances accumulated in the soil and especially in the grass, where the contamination started to be cleared only in the second half of 1987 irregularly. Air conductivities and PG were extremely high mostly in the first three months after the accident until July, after which recovery could be observed so that

normal average values returned practically by September-October, 1986 (Warzecha, 1987, 1991).

3.1.2. Measurements in Helsinki, Finland

The atmospheric electricity measurement site at Helsinki Airport is equipped with an electric field probe, a plate for measuring the atmospheric current density, and a pair of aspirators that serve the recording of air conductivity of both positive and negative polarities (Tuomi, 1982, 1988).

The arrival of the radioactive contamination at Helsinki Airport caused a gradual increase in conductivities on April 28, i.e., the second day after the accident, due to dry deposition (increase of floating) radioactive substances with the subsiding air currents. At this time the radioactive substances did not stick to the surface. This was indicated by the PG which did not decrease very much. Conductivity values went out of scales of the measurement on April 29 after a precipitation event occurred on-site. The sensitivity of the instrument was adjusted on May 2 when the conductivity was still about ten times higher than its normal level (Figure 3). At the same time, a ten- fold decrease of the PG was registered. Direct measurements of the conduction current were not available during the extreme perturbation, but the current density calculated from the electric field and conductivity, when the latter was available, shows no anomalous deviation in its general level. It was noted, however, that the time series of the current density has become noisier (Tuomi, 1989).

The suddenly appearing significant perturbation in the time series of the monitored atmospheric electricity parameters can be attributed to precipitation and the resultant significant wet deposition. The fairly quick decay of the giant peak caused by the perturbation was most probably due to the relatively quick radioactive decay of substances having short half-life (e.g., eight days for ^{131}I). The firm attachment of radionuclides to the ground at Helsinki is consistent with the wet deposition scenario because the majority of the radioactive fallout was cesium (alkali) and iodine (halogen), both of which mingle with soil minerals easily. The attachment to the ground is therefore

462 stronger by wet deposition after high-altitude transport than via dry deposition after low-
463 altitude transport of floating radioactive substances).

464 After the peak, the recovery continued on a slower rate because of radionuclides
465 which have longer half-live (e.g., 31 years for ^{137}Cs vs. eight days for ^{131}I) on one hand,
466 but also due to precipitation which washed the deposited fallout off the surface somewhat
467 deeper into the ground. Conductivity values were recovered to their normal levels
468 practically by August (Tuomi, 1989).

469

470 **3.1.3. Measurements in Uppsala, Sweden**

471

472 Conductivity, PG, and space charge measurements, complemented by recordings
473 of total radioactivity nearby in Uppsala, were running in Marsta Observatory in Sweden
474 in 1986, 1300 km away from the Chernobyl nuclear power plant. In a short publication,
475 Israelsson and Knudsen (1986) reported that the first sign of the arrival of the floating
476 radioactive substance (dry deposition) was a gradual but small increase in air
477 conductivity already on April 27, one day after the accident. The measured parameters
478 changed dramatically when light rain yielding only 0.6 mm precipitation occurred at
479 dawn of April 29. Simultaneously to the ten times increase in background radiation, air
480 conductivity increased to 11 times of its normal levels while PG decreased by a factor
481 seven. In their measurements, the space charge density also decreased by a factor of ten
482 but the authors explained it by limitations of the measurement method due to the
483 disappearing background electric field that is required in the detection method they used.

484 After a period of heavy rainfall during the days May11-13, values of the measured
485 electric parameters returned to about 40% of their normal levels. This was attributed to
486 the rain which could wash much of the depleted radioactive material deeper into the
487 ground (Israelsson and Knudsen, 1986).

488

489 **3.1.4. Measurements in Athens, Greece**

490

491 The set of observations that served the analysis in Athens, inside the city, included
492 PG measurements (at 7 m height above the ground), air conductivity measurements (only

positive polarity was available; measured at 4 m height) and small ion concentration (SIC) recordings (both polarities; detected at 4 m height). Simultaneously, activity concentration of several isotopes and the corresponding exposure rates at 1 m height were monitored at 10 km away from the AE measurement (Retalis and Pitta, 1989).

The exposure rate at the monitoring site started to increase by the evening of May 2, 1986, fully in agreement with predictions from long-range transport models according to which only the substances emitted after April 30 reached the Hellenic region. Parallel to this, air conductivity increased quickly, reaching the maximum of seven times the regular value on May 5. The simultaneous PG drop was only to 53% of its normal value, while the SIC showed four times and five times increase for positive and negative ions, respectively.

While activity concentration of the monitored isotopes at 1 m height showed a relatively fast exponential decay rate after May 2, the exposure rate maintained its level after May 5 and started to decrease slowly only after 9-10 days.. This suggests that the altitude distribution of radioactive substances varied in that time period so that a fraction of the radionuclides probably remained floating over the surface for days before they got finally deposited. In fact, the variation of atmospheric electricity parameters, which was somewhat different from the variation of the above-mentioned two parameters of radioactivity, agrees with such scenario. After the effect culminated coherently in the conductivity, PG, and SIC on May 5, a fast recovery was observed until May 8, but these parameters on May 8 still had anomalously different values compared to their regular levels. Their recovery continued, but on a much lower rate which linearly correlated with the logarithm of the activity concentration change of the monitored isotopes (Retalis, 1987; Retalis and Pitta, 1989).

Note that fair weather conditions were prevalent in Athens during the peak of the effect 3 to 7 May, and the process must be dry deposition. This is also supported by the dynamics of the changes in the AE parameters, which were more gradual and less abrupt compared to variations at the other European observation sites where the wet deposition scenario was unambiguous. The authors called the attention on that the characteristic double peak in the diurnal variation of SIC was completely masked during this period (Retalis and Pitta, 1989).

3.2. Atmospheric electrical effects detected after the accident in Fukushima

In the Fukushima accident case, long-term, one-minute resolution PG data (raw data sampling rate of 1 Hz at 2.55 m above ground) exists at Kakioka, which is located 150 km southwest from the source, and its measurement recovered from the earthquake damage just before the arrival of the radioactive substance (Takeda et al., 2011). The sensor at Kakioka uses Masacart's insulated water-dropper collector that is valid even during rainfall events with response time less than 30 s over 2000 V m^{-1} (Shigeno et al., 2001). As shown in Figure 4 (from Yamauchi et al., 2012), PG became nearly zero twice (green arrows in Figure 4), first after the surface wind from the FNPP brought the radioactive material from the source region without rain, and second after the first rain on March 20-22. The first near-zero period (starting from March 14, 2011) continued more than a day. Without firm fixation by rain during the first PG near-zero period on March 14-15, 2011, the contamination forms of the radioactive materials from the FNPP were probably suspended in the near ground air or slightly attached on the soil surface, as illustrated in the middle panel of Figure 5 (from Yamauchi et al., 2012). This means that these radioactive fallouts can easily be re-suspended by the surface wind. If the re-suspension covers all altitudes with the lowest background conductivity (e.g., < 1 km altitude), the near-surface is no longer the exception for PG altitude distribution (cf. Figure 1) where the finite PG is distributed among these altitudes, leading PG near surface to finite values. In fact the PG increased to nearly the nominal value when strong wind was observed on March 16 (cf. right panel of Figure 5), and then PG fluctuated at values 1/3 to 1/4 of the nominal values after the wind ceased until the rain was recorded (PG dropped to near-zero simultaneously). The observation during this period (from the first near-zero PG period to the first rain) shows that even the dry deposition without rain causes as quick PG drop by one order of magnitude at > 100 km distance. The observation also indicates that temporal and partial recovery of the PG must be due to re-suspension of floating radioactive materials from near the surface.

The re-suspension of radioactive materials seems to have occurred even after the wet deposition. Such re-suspension is indicated from the diurnal variation of PG (purple

arrows in Figure 4), that has different local time (LT) variation and shape from before the accident only until the diurnal variation diminished after April 20. By interpreting the diminished diurnal variation after April 20 as a firm settlement of radioactive fallout (chemical binding with soil minerals), the increase of PG near local noon during this unusual diurnal variation period can be interpreted as wide spread of high-conductance region (re-suspension of radioactive fallout) to substantial altitude, as illustrated in the right panel of Figure 5. The reason that the peak PG values do not reach as large as those of first re-suspension period (March 16-20) is because a substantial amount of surface contamination due to wet deposition (lower panel of Figure 4) makes the near surface still the highest radiation dose rate compared to the higher altitude. Such diurnal re-suspension of the radioactive materials made the surface contamination became leveled, as is seen in the radiation dose rate, which showed faster decay in the heavier contaminated area than in the lighter contaminated area (Yamauchi, 2012; Yamauchi et al., 2012). Such a leveling trend finished late April when the daily variation also diminished. Both indicate the end of substantial re-suspension from these contaminated areas. In other words, the PG data alone indicate that a substantial amount of radioactive particles were floating during the first 50 days after the Fukushima nuclear accident, and that the re-suspension diminished significantly afterward. The resultant time line of floating radionuclide flux is also confirmed by fixed sampling stations at Tsukuba and Takasaki of floating radionuclide (Stoehlker et al., 2011; Kanai, 2012), by sample measurements of floating radioactive particles (Kita et al., 2013), and by in-situ balloon measurements (Fukushima University, 2011).

Thus, PG responds differently at the different phases of the transport, fallout, re-suspension, and settlement of the radioactive materials even for the same amount of the radioactive contamination, and the PG data can be used to estimate the motion of floating radionuclides in the air. There was no clear correlation between the time profile of the PG at Kakioka and those of radiation dose rates at the near-by stations (cf. Figure 4). The minor PG changes, that reflect physical processes or dynamics of the local radioactive materials and local ions, could be interpreted by comparing the simultaneous observations of the radiation dose rates and weather records.

585 One last example of such estimate of the change in the radioactive contamination
586 condition is the rain-induced drop of radioactive materials, as indicated by yellow arrows
587 in Figure 4 (April 8 and 18). The nighttime near-zero baseline of the PG at Kakioka
588 slowly recovered during sunny days, but recovery is somewhat interrupted to set back to
589 near zero on these rainy days. Yamauchi et al. (2012) interpreted this setback as fall of
590 radionuclide from tree canopies. The radiation dose rate also shows small spikes on these
591 days, consistent with this scenario. These estimates cannot be made with the radiation
592 dose rate only. Also, high-time resolution monitoring of altitude spread is not easy with
593 the sampling method. In this sense, a combination of PG measurement and radiation dose
594 rate at weather stations is a reliable tool in monitoring the dynamics of the radioactive
595 materials such as the moment of PG drop by dry deposition and re-suspension with high
596 temporal accuracy.
597
598 **3.3. Effects of radionuclides on AE measurements under electrified cloud**
599
600 Using PG measurements alone for diagnosing conductivity enhancements has
601 some limitations: other electric charges, such as cloud electricity, also influence PG in the
602 atmosphere, and mostly the fair weather conditions have been examined until recently.
603 The reason for using PG, despite this problem, to diagnose the electric conductivity is
604 that the electric conductivity is not easy to measure for very low conductivity in the
605 neutral atmosphere. Recently, Yamauchi et al. (2018) found a symptom of PG change
606 even under rain conditions that gives some idea on conductivity and floating
607 radionuclides as described below, although the effect is yet to be quantified.
608 Before the FNPP accident, PG data during the fine weather condition only were
609 analyzed. Data from Kakioka opened new possibility in analyzing the PG data during
610 rain, although the effect of the increased radioactive dust in the atmosphere was identified
611 only in statistics. The difficulty in identifying the effect of increased radiation dose rate in
612 the air under the electrified cloud mainly comes from quick PG changes within a few
613 minutes, as shown in the upper panel of Figure 6 (from Yamauchi et al., 2018), PG
614 decays quickly from its negative peaks corresponding to negative charges that are
615 accumulated at the lower part of the electrified cloud. In the figure, averaged time

profiles from the negative PG peak (peak values are between -200 to -400 V m^{-1}) shows shorter time constants for the first 50 days after the Fukushima nuclear accident than the same period of the other years, while no difference was seen before or after this 50-days period. The observed shortening of the time scale is symmetric between rising and decay.

The observations can be attributed to the electrostatic shielding effect of the cloud charges by the enhanced ionization as illustrated in the lower panels of Figure 6. For positive peaks, no notable difference was detected on the time scale to/from the peak between 2011 and the other years. This is consistent with the concentration of the radioactive particle at low altitude (< 500 m according to in-situ gamma ray observations by radiosonde), where negative cloud charges exceed the positive charges. The PG data under electrified cloud gives additional information on the altitude range of the re-suspended radioactive fallouts. The results open up a new possibility to use PG as an independent monitor of radioactivity at some altitudes even during long period of cloudy/rainy conditions.

3.4. Indirect effects of radionuclides on AE measurements

Radionuclides released to the atmosphere get attached to aerosols which can further influence different atmospheric processes, and transport dynamics of radioactive aerosols can be different from the normal case. Aerodynamic size and hygroscopicity are the two most important microphysical properties of aerosols, which determine atmospheric lifetime and deposition amounts. The modeling studies following Fukushima accident pointed out that knowledge of these aerosol properties is just as important as the accuracy of the meteorological simulations and emission scenarios (Saito et al., 2015). Radioactive particles influence charge transfer processes within the clouds through ion-induced aerosol particle formation (Williams and Mareev, 2014). In fact, enhanced thunderstorm activity and higher occurrence of lightning in Sweden after the Chernobyl accident can be explained by the increased radioactivity (Israelsson et al., 1987), although the observed increase of 30% may simply be due to annual anomaly. The influences may thus be diverse and are supposed to depend on a large number of factors, e.g., physical and chemical characteristics of radionuclides, size and density of the radioactive plume,

distribution of atmospheric pressure, general atmospheric circulation, local winds, weather conditions at the time of the accident, altitude of the emitting source, regional ocean currents, thermohaline circulation, and regional as well as global climate anomalies.

4. Discussion

Recognizing the need to improve the understanding of processes governing radionuclide behavior in the environment, both accidents led to the revival of research on preparing for similar scenarios in the future. Following the Chernobyl accident, a number of decision-supporting models have been developed. These models incorporated information on factors which influence the concentration of airborne radionuclides. Meteorological data, dry and wet deposition processes and orographic data were considered. In the decades that followed, the focus was more on dispersion models which vary in terms of their structure, specific output, spatial scale and complexity. They aimed at providing predictions for atmospheric dispersion to support emergency response in accidental releases. Such predictions of atmospheric dispersion assuming point unit source were actually issued on the web by different teams after the accident in Fukushima, e.g., by Norway, Austria, France, and Germany, but measurement-based open warning was not provided due to the lack of sufficient active monitoring stations, particularly for the floating radioactive materials in the air.

Airborne radionuclides from the considered nuclear accidents significantly perturbed the electrical characteristics of air and thus contributed significantly to research on the atmospheric electricity. AE-related effects of the Chernobyl accident were reported from a very wide region even from over 1000 km distance in countries in North-East, East, and South-East Europe. A variety of atmospheric electricity measurements were running at the different monitoring stations. These monitoring capabilities include PG and air conductivity measurements at all stations, with additional complete observations of space charge and atmospheric current density, aerosols, condensation nuclei and small ion concentration at some stations. Being aware of the importance of wet deposition of airborne radioactive material, various sets of meteorological data were

678 incorporated in studies. Nuclear-accident-related studies also considered various
679 reference measurements of exposure rates or environmental radioactivity (usually from
680 the nearest monitoring site) in the form of fallout activity concentration at ground or near
681 the surface in the air.

682 Such rich set of measurements allowed the examination of the response of
683 various parameters of atmospheric electricity to the Chernobyl-origin nuclear substances
684 that arrived at the region in the air. Air conductivity was found to be more sensitive to
685 radioactive contamination than the PG at most sites. The ratio of the change rate in air
686 conductivity to that in PG were 3.0 (10/3.33) in Poland, 1.57 (11/7) in Sweden, 3.7
687 (7/1.89) in Greece, and 1.0 (10/10) in Finland. On one hand, variation of this ratio can be
688 attributed to local factors affecting the sensitivity of the measurements. For example,
689 conductivity and PG measurements in Athens were made at different heights. On the
690 other hand, the vertical distribution of the radionuclides in the air and the type of the
691 deposition (wet or dry) also has an influence on this ratio. While all measured
692 atmospheric electricity parameters were affected by the perturbation caused by the
693 elevated level of radioactivity in the air, the effect on the electric current density in the air
694 was found to be very small (only some increased noise was measured in Finland). This
695 suggests that the large-scale GEC was not affected despite the dramatic changes in the
696 local electric properties of the environment.

697 In addition to the observation of fundamental effects, i.e., increasing conductivity
698 and decreasing PG, several observations were made after the Chernobyl accident on the
699 interconnections within a larger set of atmospheric electricity parameters, aerosol as well
700 as ion concentration variations. However, perturbations manifested in specific variations
701 in the composition and size of ions and aerosols could be observed at limited sites where
702 the corresponding measurements were available. This resulted in that some observations
703 could not be confirmed by independent measurements. Such unconfirmed observations
704 include the anomalously higher conductivity of negative ions compared to that of positive
705 ones in Poland, the unexpected decrease in space charge density recorded in Sweden, or
706 the characteristic change in the diurnal variation of small ion concentration detected in
707 Greece. On the other hand, the hypothesis on the observed lowered concentration of
708 condensation nuclei in Poland (i.e., that mostly small ions were produced) was indirectly

supported by the measured (and slightly asymmetric) growth of positive and negative small ion concentrations noted in Greece. These experiences underline the importance of running as many different measurements at an observation site as possible.

For Fukushima accident, such multi-point comparison was not possible partly because the radionuclides spread mainly over ocean where no observatory exists, and Kakioka without conductivity measurements was the only PG station that was active within the affected area. On the other hand, there was a dense network of the meteorological monitoring sites. Therefore, atmospheric electricity-related studies on the Fukushima accident concentrated only on the PG and discuss its local variation in detail together with the variation of meteorological parameters (i.e., rain and wind) as well as radiation dose rate from a nearby monitoring site. The high time resolution (10 min) meteorological records and radiation dose rate allowed making detailed studies of the changing effect of dry deposition for several days. In these studies, the emphasis was placed on identifying as many factors as possible from those which drive the variations of PG in association with the environmental changes caused by the arriving nuclear contamination in the air. Dry deposition scenarios were present in Poland and in Greece, too, after the Chernobyl accident, but the discussion in the corresponding papers focused more on the responses of the various measured atmospheric electricity parameters to the radioactive material and not very specifically behaviors of arrived radioactive material such as re-suspension and its relation to meteorological parameters. In studies associated with the accident in Chernobyl, the primary role of meteorological data was to confirm fair weather conditions and precipitation events.

The analyses based on PG measurements in Kakioka could benefit from the sequence of rain events causing wet deposition after the days of dry deposition/re-suspension period. In this way, both dry and wet deposition scenarios were studied. Furthermore, partial re-suspension of the wet-deposited radioactive material could be recognized. Note that a similar sequence of dry and wet deposition scenarios also happened in Sweden and Finland after the Chernobyl accident but the length of the dry deposition periods was only one-two days in both cases and detailed analysis on the PG variations in connection with the changing weather conditions was not published. Correspondences between PG variations and meteorological conditions, transport,

settlement, and fallout processes are known much better nowadays as a result of extensive studies in connection with the Fukushima event.

5. Conclusions

Contribution of studies on the electrical environment to know the time evolution of the state and properties of radioactive contamination, which has primary importance for predicting, estimating, and surveying the consequences of large-scale emission events of radioactive substance, were reviewed in this study. Main findings are found after Chernobyl and Fukushima nuclear accidents. AE-related studies published in connection with the Chernobyl accident compared the temporal variations of various, locally measured AE parameters either to one-another and to local measurements of radioactivity when those were available. While effects of radionuclides from Fukushima on the electrical properties of the atmosphere have been investigated by focusing on PG measurements, meteorological conditions were more carefully considered than in earlier studies and the potential of PG measurements was demonstrated in differentiating between events of dry and wet deposition as well as re-suspension of the airborne radioactive material.

According to measurements after these accidents, air conductivity seems to be the most sensitive AE parameter from the point of view of detecting the local effects of airborne radionuclides, whereas the atmospheric electric current density was fairly stable during the episodes of radioactive contamination. This suggests that, PG can be used to indicate the changes in air conductivity through Ohm's law, and that the overall state of the GEC is not changed significantly (at least on short terms) because of the intake of radionuclides in the atmosphere. Despite this finding, the ratio between the change rates of air conductivity and PG varied significantly (1.0-3.7) at different observation sites. Characteristics of the local measuring environment may contribute to this variation, the origin of which remains to be identified yet.

According to the experience from Athens after the Chernobyl accident, also the concentration of small ions is sensitive to the appearance of airborne radionuclides, but measuring it is not easy compared to the monitoring of PG. Space charge measurements,

771 as they were implemented in Sweden, could not indicate radioactivity-related effects
772 unambiguously. Similarly, variations of the aerosol concentration alone are not suitable
773 for detecting the arrival of radioactive contamination at the monitoring site. These
774 measurements must be evaluated together with records of proven indicator parameters.
775 Studies in connection with the Fukushima event clearly demonstrated that PG is a
776 very useful and convenient parameter for studying the effects of nuclear contamination in
777 the atmosphere. Not only it is apparently easy to measure, but its variation was found to
778 mirror the characteristics of vertical transport processes and the changes in the local
779 distribution of the radioactive material, for which no other remote sensing method is
780 found. PG can be used to distinguish between wet and dry deposition scenarios and to
781 detect re-suspension of radionuclides from the ground (even after wet deposition).
782 Perturbations and smoothing of the diurnal PG variation refer to redistributions of the
783 radioactive material in the environment corresponding to its falling from tree canopies or
784 altitude spreading of the contaminated air layer, respectively. Thus, PG measurement,
785 together with radiation dose rate measurement, constructs a unique method to monitor
786 floating radionuclides at more than 10 m altitude, which is not possible to measureby
787 other ground-based methods. Therefore, PG stations are a good infrastructure to deploy
788 around nuclear facilities.
789 The dynamics of the changes registered in PG or in air conductivity can be used to
790 infer variations in the composition and amount of radioactive material deposited on the
791 surface of the ground. The ratio of radioactive components with different half-time can be
792 inferred from the recovery rate of those AE parameters in the local environment. On
793 longer terms, recovery and clearing of the ground from radionuclides can be monitored
794 the same way. Note that the change reflected by the variation of AE parameters was
795 found to be different from what had been obtained by direct measurements of near-
796 surface exposure and activity concentration.
797 These experiences indicate well that AE measurements could be used to verify and
798 support models on atmospheric transport, distribution, and the composition of clouds of
799 radionuclides. On the other hand, the corresponding direct isotope measurements and
800 model outputs can be used to interpret the details of the observed variations of AE
801 parameters. Some of the most widely used transport and dispersion models are briefly

reviewed in section 2 of this study for consideration in planning future research on the subject.

A unique benefit of AE measurement is that they can serve studies on microphysical effects of airborne radioactivity. Aerosol and small ion measurements and detection of space charge density at some of the observation sites revealed asymmetry in ionization and attachment processes in terms of the polarity of the involved particles in response to increased radioactivity in air. Several corresponding results need to be confirmed yet either by modeling or by other measurements. In any case, these results emphasize that it is worth equipping atmospheric electricity monitoring sites with a more complete set of instrumentation. Measuring atmospheric conductivity in addition to PG and a well-equipped meteorological station is particularly suggested.

Results on the responses of atmospheric electricity parameters to nuclear substances carried with the air in case of both Chernobyl and Fukushima demonstrate well the high potential of atmospheric electricity measurements in detecting and monitoring the presence of radioactive material in the atmosphere. A novel approach indicates that PG measurements are capable of fulfilling this task not only in fair weather but also in the presence of clouds.

Acknowledgements

The authors SD, JP, MĆ, RD, MĐ and JB would like to acknowledge networking support by the COST Action CA15211. The authors SD, JP, MĆ, RD and MĐ acknowledge the support of the Ministry of Education, Science and Technological Development of the Republic of Serbia (project III43009). MK was supported by the Japanese Radioactivity Survey from the NRA, Japan, the Japan Society of the Promotion of Science (JSPS) and Ministère des Affaires Étrangères et du Développement International (MAEDI) under the Japan - France Integrated Action Program (SAKURA), and the Environmental Research and Technology Development Fund of the Environmental Restoration and Conservation Agency (ERCA) (1-1802). MA was supported in part by the radioactive survey and the research fund of the Ministry of Education, Culture, Sports, Science and Technology (MEXT), Japan (Houshanou-chousa-kenkyuhi, FY2011–2014) and in part by the J-RAPID fund of the Japan Science and Technology Agency for the project entitled “Investigation and Prediction of Impacts of the 2011 off the Pacific coast of Tohoku Earthquake on Marine Environment, FY2011–2012”. MA was also supported by research fund of Institute of Environmental Radioactivity, Fukushima University, during the period from FY2014 to FY2018, too. Contribution of JB was supported by the National Research, Development and Innovation Office, Hungary-NKFIH, K115836. The atmospheric electricity (PG) data at Kakioka and

relevant weather data are provided by the Japan Meteorological Agency and publicly available at http://www.kakioka-jma.go.jp/obsdata/metadata/en/ and http://www.data.jma.go.jp/gmd/risk/obsdl/index.php. The radiation dose rate data is provided by Ibaraki-ken prefecture.

References

Adachi, K., Kajino, M., Zaizen, Y., Igarashi, Y., 2013. Emission of spherical cesium-bearing particles from an early stage of the Fukushima nuclear accident. Sci. Rep. 3: 2554. https://doi.org/10.1038/srep02554.

Aoyama, M., Tsumune, D., Inomata, Y., Tateda, Y., 2020. Mass balance and latest fluxes of radiocesium derived from the Fukushima accident in the western North Pacific Ocean and coastal regions of Japan, J. Environ. Radioact. 217, 106206. https://doi.org/10.1016/j.jenvrad.2020.106206.

Aoyama, M., Hamajima, Y., Hult, M., Oka, E., Tsumune, D., Kumamoto, Y., 2016a. ^{134}Cs and ^{137}Cs in the North Pacific Ocean derived from the March 2011 TEPCO Fukushima Dai-ichi Nuclear Power Plant accident, Japan. Part one: surface pathway and vertical distributions, J. Oceanogr. 72, 53-65. doi: 10.1007/s10872-015-0335-z.

Aoyama, M., Kajino, M., Tanaka, T.Y., Sekiyama, T.T., Tsunume, D., Tsubono, T., Hamajima, Y., Inomata, Y., Gamo, T., 2016b. ^{134}Cs and ^{137}Cs in the North Pacific Ocean derived from the March 2011 TEPCO Fukushima Dai-ichi Nuclear Power Plant accident, Japan. Part two: estimation of ^{134}Cs and ^{137}Cs inventories in the North Pacific Ocean, J. Oceanogr. 72, 67-76. https://doi.org/10.1007/s10872-015-0332-2.

Aoyama, M., Uematsu, M., Tsumune, D., Hamayima, Y., 2013. Surface pathway of radioactive plume of TEPCO Fukushima NPP1 released ^{134}Cs and ^{137}Cs, Biogeosciences, 10, 3067-3078. https://doi.org/10.5194/bg-10-3067-2013.

ApSimon H.M., Wilson, J.J.N., 1987. Modelling atmospheric dispersal of the Chernobyl release across Europe. Boundary Layer Meteor. 41, 123-133. https://doi.org/10.1007/BF00120435.

ApSimon, H.M., Goddard A.J.H., Wrigley J., 1985. Long-range atmospheric dispersion of radioisotopes – i. the MESOS model. Atmos. Environ. 19, 99-111. https://doi.org/10.1016/0004-6981(85)90141-6.

Bedwell, P., Wellings, J., Leadbetter, S., Tomas, J., Andronopoulos, S., Korsakissok, I., Périllat, R., Mathieu, A., Geertsema, G., Klein, H., de Vries, H., Hamburger, T., Pázmándi, T., Rudas, C., Sogachev, A., Szántó, P., 2018. Guidelines detailing the range and distribution of atmospheric dispersion model input parameter uncertainties. In: Guidelines ranking uncertainties for atmospheric dispersion European joint programme for the integration of radiation protection research.

Benamrane, Y., Wybo, J.-L., Armand, P., 2013. Chernobyl and Fukushima nuclear accidents: what has changed in the use of atmospheric dispersion modeling? J. Environ. Radioact. 126, 239-252. https://doi.org/10.1016/j.jenvrad.2013.07.009.

Bennett, A.J., Harrison, R.G., 2008, Variability in surface atmospheric electric field measurements. J. Phys. Conf. Ser. 142, 012046IOP. https://doi.org/10.1088/1742-6596/142/1/012046.

884 Beresford N., Fesenko S, Konoplev A, Skuterud L, Smith J.T., Voigt G, 2016. Thirty
885 years after the Chernobyl accident: What lessons have we learnt? J. Environ.
886 Radioact. 157, 77-89. https://doi.org/10.1016/j.jenvrad.2016.02.003.
887 Bonjean, F., Lagerloef, G.S.E., 2002. Diagnostic model and analysis of the surface
888 currents in the tropical Pacific Ocean. J. Phys. Oceanogr. 32, 2938–2954.
889 https://doi.org/10.1175/1520-0485(2002)032<2938:DMAAOT>2.0.CO;2.
890 Buesseler, K., Aoyama, M., Benitez-Nelson, K., Charmasson, S., Higley, K., Maderich,
891 V., Masqué, P., Morris, P.J., Oughton, D., Smith, J.N., 2017. Fukushima Daiichi–
892 Derived Radionuclides in the Ocean: Transport, Fate, and Impacts. Ann. Rev.
893 Mar. Sci. 9, 173-203. https://doi.org/10.1146/annurev-marine-010816-060733.
894 Chang, C.-C., Burr, G.S., Jull, A.J.T., Russell, J., Priyadarshi, A., Lin, M., Thiemens, M.,
895 Biddulph, D., 2019. Measurements of ^{129}I in the Pacific Ocean at Scripps Pier and
896 Pacific Northwest sites: A search for effects from the 2011 Fukushima Daiichi
897 Nuclear Power Plant accident and Hanford. Sci. Total Environ. 689, 1023-1029.
898 https://doi.org/10.1016/j.scitotenv.2019.06.372.
899 Chino, M., Nakayama, H., Nagai, H., Terada, H., Katata, G., Yamazawa, H., 2011.
900 Preliminary estimation of release amounts of ^{131}I and ^{137}Cs accidentally
901 discharged from the Fukushima Daiichi nuclear power plant into the atmosphere.
902 J. Nucl. Sci. Technol. 48, 1129-1134.
903 https://doi.org/10.1080/18811248.2011.9711799.
904 Crandall, W.K., Molenkamp, C.R., Williams, A.L., Fulk, M.M., Lange, R., Knox, J.B..
905 1973. An Investigation of scavenging of radioactivity from nuclear debris clouds:
906 research in progress, Lawrence Livermore Laboratory Report, UCRL-51328,
907 https://inis.iaea.org/collection/NCLCollectionStore/_Public/04/068/4068239.pdf.
908 CTBTO (Comprehensive Nuclear-Test-Ban Treaty Organization), 2011. Fukushima
909 Related Measurements by the CTBTO. [Online] Available at:
910 http://www.ctbto.org/press-centre/highlights/2011/fukushima-related-
911 measurements-bythe-ctbto/fukushima-related-measurements-by-the-ctbto-page-1/.
912 De Cort, M., Dubois, G., Fridman, S.D., Germenchuk, M.G., Izrael, Y.A., et al., 1998.
913 Atlas of Caesium Deposition on Europe after the Chernobyl Accident. Office for
914 Official Publications of the European Communities, Luxembourg. ISBN 92-828-
915 3140-X.
916 Dragović, S., Howard, B.J., Caborn, J.A., Barnett, C.L., Mihailović, N., 2010. Transfer of
917 natural and anthropogenic radionuclides to ants, bryophytes and lichen in a semi-
918 natural ecosystem. Environ. Monit. Assess. 166, 677-686.
919 https://doi.org/10.1007/s10661-009-1032-4.
920 Draxler, R., Arnold, D., Chino, M., Galmarini, S., Hort, M., Jones, A., Leadbetter, S.,
921 Malo, A., Maurer, C., Rolph, G., Saito, K., Servranckx, R., Shimbori, T., Solazzo,
922 E., Wotawa, G., 2015. World Meteorological Organization's model simulations of
923 the radionuclide dispersion and deposition from the Fukushima Daiichi nuclear
924 power plant accident. J. Environ. Radioact. 139, 172-184.
925 https://doi.org/10.1016/j.jenvrad.2013.09.014.
926 Ellis J., 2003. Use of atmospheric models in response to the Chernobyl disaster, in:
927 Tracking and Predicting the Atmospheric Dispersion of Hazardous Material
928 Releases: Implications for Homeland Security. Committee on the Atmospheric

Dispersion of Hazardous Material Releases, National Research Council, pp. 87-88.

Evangeliou, N., Balkanski, Y., Cozic, A., Møller A.P., 2013a. Global transport and deposition of ^{137}Cs following the Fukushima Nuclear Power Plant Accident in Japan: Emphasis on Europe and Asia using high-resolution model versions and radiological impact assessment of the human population and the environment using interactive tools. Environ. Sci. Technol. 47, 5803-5812. https://doi.org/10.1021/es400372u.

Evangeliou, N., Balkanski, Y., Cozic, A., Møller, A.P., 2013b. Simulations of the transport and deposition of ^{137}Cs over Europe after the Chernobyl Nuclear Power Plant accident: influence of varying emission-altitude and model horizontal and vertical resolution. Atmos. Chem. Phys. 13, 7183-7198. https://doi.org/10.5194/acp-13-7183-2013.

Evangeliou, N., Hamburger, T., Talerko, N., Zibtsev, S., Bondar, Y., Stohl, A., Balkanski, Y., Mousseau, T.A., Møller, A.P., 2016. Reconstructing the Chernobyl Nuclear Power Plant (CNPP) accident 30 years after. A unique database of air concentration and deposition measurements over Europe. Environ. Pollut. 216, 408-418. https://doi.org/10.1016/j.envpol.2016.05.030.

Fukushima University (2011) press release, 11 May, 2011. http://www.sss.fukushima-u.ac.jp/sonde_data.

Haldoupis, C., Rycroft, M. Williams, E., Price, C., 2017. Is the "Earth-ionosphere capacitor" a valid component in the atmospheric global electric circuit? J. Atmos. Sol-Terr. Phy., 164, 127-131. https://doi.org/10.1016/j.jastp.2017.08.012.

Hamilton, R.A., Paren, J.G., 1967. The influence of radioactive fallout on the atmospheric potential gradient. Meteorol. Mag. 96, 81-85.

Harris, D.L., 1955. Effects of radioactive debris from nuclear explosions on the electrical conductivity of the lower atmosphere. J. Geophys. Res. 60, 45-52. https://doi.org/10.1029/JZ060i001p00045.

Harrison R.G., Nicoll K.A., 2018. Fair weather criteria for atmospheric electricity measurements. J. Atmos. Sol. Terr. Phys. 179, 239-250. https://doi.org/10.1016/j.jastp.2019.01.003.

Harrison, R. G., Carslaw, K. S., 2003. Ion-aerosol-cloud processes in the lower atmosphere. Rev. Geophys. 41. https://doi.org/10.1029/2002RG000114.

Harrison, R.G., 2003. Twentieth century atmospheric electrical measurements at the observatories of Kew, Eskdalemuir and Lerwick. Weather 58, 11-19. https://doi.org/10.1256/wea.239.01.

Harrison, R.G., Bennett, A.J., 2007. Cosmic ray and air conductivity profiles retrieved from early twentieth century balloon soundings of the lower troposphere. J. Atmos. Sol. Terr. Phys. 69, 515–527. 10.1016/j.jastp.2006.09.008.

Harrison, R.G., Ingram, W.J., 2005. Air-earth current measurements at Kew, London, 1909-1979. Atmos. Res. 76, 49-64. https://doi.org/10.1016/j.atmosres.2004.11.022.

Hass, H., Memmesheimer, M., Geiβ, H., Jakobs, H.J., Laube, M., Ebel, A., 1990. Simulation of the Chernobyl radioactive cloud over Europe using the Eurad model. Atmos. Environ. 24, 673-692. https://doi.org/10.1016/0960-1686(90)90022-F.

Honda, M.C, Aono, T., Aoyama, M., Hamajima, Y, Kawamaki, H., Kitamura, M., Masumoto, Y., Miyazawa, Y., Takigawa, M., Saino, T., 2012. Dispersion of artificial caesium-134 and-137 in the western North Pacific one month after the Fukushima accident. Geochem. J. 46, e1-e9. https://doi.org/10.2343/geochemj.1.0152.

Huang, D., Lin, J., Du, J., Yu, T., 2020. The detection of Fukushima-derived radiocesium in the Bering Sea and Arctic Ocean six years after the nuclear accident. Environ. Pollut. 256, 113386, https://doi.org/10.1016/j.envpol.2019.113386.Huzita A., 1966. Effect of Radioactive Fallout Upon the Electrical Conductivity of the Lower Atmosphere. J. Geomagn. Geolectr. 18, 363-372. https://doi.org/10.5636/jgg.18.363.

IAEA (International Atomic Energy Agency), 2006. Environmental consequences of the Chernobyl accident and their remediation: twenty years of experience / report of the Chernobyl, Forum Expert Group "Environment", IAEA, Vienna, Austria, ISBN 92–0–114705–8.

IAEA (International Atomic Energy Agency), 2015. The Fukushima Daiichi Accident, IAEA, Vienna, Austria, ISBN 978–92–0–107015–9.

IEM (Iowa Environmental Mesonet), http://mesonet.agron.iastate.edu/sites/windrose.phtml?network=JP__ASOS&station=RJSS.

Inomata, Y., Aoyama, M., Hirose, K., Sanada, Y., Torii, T., Tsubono, T., Tsunume, D., Yamada, M., 2014. Distribution of radionuclides in surface seawater obtained by an aerial radiological survey. J. Nucl. Sci. Technol. 51, 1059-1063. https://doi.org/10.1080/00223131.2014.914451.

Inomata, Y., Aoyama, M., Tsubono, T., Tsumune, D., Hirose, K., 2016. Spatial and temporal distributions of ^{134}Cs and ^{137}Cs derived from the TEPCO Fukushima Daiichi Nuclear Power Plant accident in the North Pacific Ocean by using optimal interpolation analysis. Environ. Sci. Proc. Imp. 18, 126-36. DOI:10.1039/C5EM00324E.

Israelsson, S, Knudsen, E, 1986. Effect of radioactive fallout from a nuclear power plant accident on electrical parameters. J. Geophys. Res. 91, 11909-11910. https://doi.org/10.1029/JD091iD11p11909.

Israelsson, S., Shutte, T., Pisler, E., Lundquist, S., 1987. Increased occurrence of lightning flashes in Sweden during 1986. J. Geophys. Res. 92, 10996–10998. https://doi.org/10.1029/JD092iD09p10996.

Jana, S., Maitra, A., 2019, Electric field variation in clear and convective conditions at a tropical urban location. J. Geophys. Res. Atmos. 124, 2068– 2078. https://doi.org/10.1029/2018JD028310.

Kajino, M., Sekiyama, T.T., Igarashi, Y., Katata, G., Sawada, M., Adachi, K., Zaizen, Y., Tsuruta, H., Nakajima, T., 2019. Deposition and Dispersion of Radio-Cesium Released Due to the Fukushima Nuclear Accident: Sensitivity to Meteorological Models and Physical Modules. J. Geophys. Res. Atmos. 124, 1823-1845. https://doi.org/10.1029/2018JD028998.

Kanai, Y., 2012. Monitoring of aerosols in Tsukuba after Fukushima Nuclear Power Plant incident in 2011. J. Environ. Radioact. 111, 33-37. DOI:10.1016/j.jenvrad.2011.10.011.

Katata, G., Chino, M., Kobayashi, T., Terada, H., Ota, M., Nagai, H., Kajino, M., Draxler, R., Hort, M.C., Malo, A., Torii, T., Sanada, Y., 2015. Detailed source term estimation of the atmospheric release for the Fukushima Daiichi Nuclear Power Station accident by coupling simulations of an atmospheric dispersion model with an improved deposition scheme and oceanic dispersion model. Atmos. Chem. Phys. 15, 1029-1070. https://doi.org/10.5194/acp-15-1029-2015.

Katata, G., Ota, M., Terada, H., Chino, M., Nagai, H., 2012. Atmospheric discharge and dispersion of radionuclides during the Fukushima Daiichi Nuclear Power Plant accident. Part I: source term estimation and local-scale atmospheric dispersion in early phase of the accident. J. Environ. Radioact. 109, 103-113. https://doi.org/10.1016/j.jenvrad.2012.02.006.

Kawano, M., Ikebe, Y., Shimo, M., 1969. Measurements of attachment coefficients of small ions and radioactive ions to condensation nuclei, in: Coroniti, S., Hughes J. (Eds.), Planetary Electrodynamics, Gordon and Breach, New York, 1, pp. 136-154.

Kita K, Kasahara R, Tanaka M, Sato K, Demizu H, et al., 2013. Variation of atmospheric concentrations of I-131, Cs-134 and Cs-137 observed over eastern Japan: contribution of leakage from Fukushima Dai-ichi Nuclear Power Plant and secondary emission from soil and vegetation. Geophys. Res. Abstr. 15, EGU2013-5090.

Kondo G., 1959. The Recent Status of Secular Variation of the Atmospheric Electric Elements and their Relation to the Nuclear Explosions, Memoirs of Kakioka Magnetic Observatory, 9, 2-6.

Koo, Y.-H., Yang, Y.-S., Song, K.-W., 2014. Radioactivity release from the Fukushima accident and its consequences: A review. Prog. Nucl. Energ 74, 61-70. https://doi.org/10.1016/j.pnucene.2014.02.013.

Korobova, E., Linnik, V., Chizhikova, N., 2008. The history of the Chernobyl ^{137}Cs contamination of the flood plain soils and its relation to physical and chemical properties of the soil horizons (a case study). J. Geochem. Explor. 96, 236-255. https://doi.org/10.1016/j.gexplo.2007.04.014.

Korsakissok, I., Mathieu, A., Didier, D., 2013. Atmospheric dispersion and ground deposition induced by the Fukushima Nuclear power plant accident: a local-scale simulation and sensitivity study. Atmos. Environ. 70, 267-279. https://doi.org/10.1016/j.atmosenv.2013.01.002.

Kumamoto, Y., Aoyama, M., Hamajima, Y., Nishino, S., Murata, A., Kikuchi, T., 2016. Meridional distribution of Fukushima-derived radiocesium in surface seawater along a trans-Pacific line from the Arctic to Antarctic Oceans in summer 2012. J. Radioanal. Nucl. Chem. 307, 1703-1710. https://doi.org/10.1007/s10967-015-4439-0.

Kumamoto, Y., Aoyama, M., Hamajima, Y., Nishino, S., Murata, A., Kikuchi, T., 2017. Radiocesium in the western subarctic area of the north Pacific Ocean, Bering Sea, and Arctic Ocean in 2013 and 2014. Appl. Radiat. Isot. 126, 88-92. https://doi.org/ 10.1016/j.apradiso.2017.02.036.

Kumamoto Y, Aoyama M, Hamajima Y, Nishino S, Murata A, Kikuchi T., 2019. Radiocesium in the western subarctic area of the North Pacific ocean, Bering Sea,

and Arctic Ocean in 2015 and 2017. Polar Science 2019; 21: 228-232. https://doi.org/10.1016/j.polar.2018.08.007.
Leelőssy, Á., Lagzi, I., Kovács, A., Mészáros, R., 2018. A review of numerical models to predict the atmospheric dispersion of radionuclides. J. Environ. Radioact. 182, 20-33. https://doi.org/10.1016/j.jenvrad.2017.11.009.
Lelieveld J., Kunkel D, Lawrence M.G., 2012. Global risk of radioactive fallout after major nuclear accidents. Atmos. Chem. Phys. 12, 4245-4258. DOI:10.5194/acp-12-4245-2012.
Lin, W., Chen, L., Yu, W., Ma, H., Zeng, Z., Lin, J., Zeng, S., 2015. Radioactivity impacts of the Fukushima Nuclear Accident on the atmosphere. Atmos. Environ. 102, 311-322. https://doi.org/10.1016/j.atmosenv.2014.11.047.
Marzo, G.A., 2014. Atmospheric transport and deposition of radionuclides released after the Fukushima Dai-chi accident and resulting effective dose. Atmos. Environ. 94, 709-722. https://doi.org/10.1016/j.atmosenv.2014.06.009.
Mathieu, A., Kajino, M., Korsakissok, I., Périllat, R., Quélo, D., Quérel, A., Saunier, O., Sekiyama, T.T., Igarashi, Y., Didier, D., 2018. Fukushima Daiichi–derived radionuclides in the atmosphere, transport and deposition in Japan: A review. Appl. Geochem. 91, 122-139. https://doi.org/10.1016/j.apgeochem.2018.01.002.
MEXT (Ministry of Education, Culture, Sports, Science and Technology), 2007. SPEEDI System for Prediction of Environmental Emergency Dose Information, Pamphlet of SPEEDI.
MEXT (Ministry of Education, Culture, Sports, Science and Technology), 2011. Results of Airborne Monitoring by the Ministry of Education, Culture, Sports, Science and Technology and the U.S. Department of Energy, Annex 1, https://radioactivity.nsr.go.jp/en/contents/4000/3180/24/1304797_0506.pdf.
Morino, Y., Ohara, T., Nishizawa, M., 2011. Atmospheric behavior, deposition, and budget of radioactive materials from the Fukushima Daiichi nuclear power plant in March 2011. Geophys. Res. Lett. 38. https://doi.org/10.1029/2011GL048689.
Morino, Y., Ohara, T., Watanabe, M., Hayashi, S., Nishizawa, M., 2013. Episode analysis of deposition of radiocesium from the Fukushima Daiichi nuclear power plant accident. Environ. Sci. Technol. 47, 2314-2022. https://doi.org/10.1021/es304620x.
Nagai, H., Chino, M., Yamazawa, H., 1999. Development of scheme for predicting atmospheric dispersion of radionuclides during nuclear emergency by using atmospheric dynamic model. J. At. Energy. Soc. Jpn. 41, 777–785, [in Japanese with English abstract].
Nakajima, T., Misawa, S., Morino, Y., Tsuruta, H., Goto, D., Uchida, J., Takemura, T., Ohara, T., Oura, Y., Ebihara M., Satoh, M., 2017. Model depiction of the atmospheric flows of radioactive cesium emitted from the Fukushima Daiichi Nuclear Power Station accident. Prog. Earth Planet. Sci. 4, 2. https://doi.org/10.1186/s40645-017-0117-x.
Nicoll, K.A., 2012. Measurements of atmospheric electricity aloft. Surv. Geophys. 33, 991-1057. https://doi.org/10.1007/s10712-012-9188-9.
Nicoll, K. A., R. G. Harrison, V. Barta, J. Bor, R. Brugge, A. Chillingarian, J. Chum, A. K. Georgoulias, A. Guha, K. Kourtidis, M. Kubicki, E. Mareev, J. Matthews, H. Mkrtchyan, A. Odzimek, J.-P. Raulin, D. Robert, H. G. Silva, J. Tacza, Y. Yair,

and R.Yaniv, 2019, A global atmospheric electricity monitoring network for climate and geophysical research, J. Atmos. Sol-Terr. Phy., 184, 18-29. https://doi.org/10.1016/j.jastp.2019.01.003.

Ogawa T., Morita M., 1977. Electric conductivity, ozon concentration, water vapour pressure, and electric current at 20-350mb altitude (in Japanese), Taiki-Denki Kenkyu (Proceedings of the Society of Atmospheric Electricity of Japan), 18, 107-114, doi:10.11501/9666801, ISSN 0286-3405. http://dl.ndl.go.jp/info:ndljp/pid/9666801.

Panitz, H.-J., Matzerath, C., Päsler-Sauer J., 1989. UFOMOD Atmospheric Dispersion and Deposition, Institut für Neutronenphysik und Reaktortechnik Projekt LWR-Sicherheit, KfK 4332, ISSN 0303-4003.

Pierce, E.T., 1959. Some calculations on radioactive fallout with especial reference to the secular variations in potential gradient at Eskdalemuir, Scotland. Pure Appl. Geophys. 42, 145-151. https://doi.org/10.1007/BF02113404.

Pierce, E.T., 1972. Radioactive fallout and secular effects in atmospheric electricity. J. Geophys. Res. 77, 482-487. https://doi.org/10.1029/JC077i003p00482.

Piper, I. M., Bennett. A. J., 2012. Observations of the atmospheric electric field during two case studies of boundary layer processes. Environ. Res. Lett. 7, 014017. https://doi.org/10.1088/1748-9326/7/1/014017.

Povinec, P.P., Gera, M., Holy, K., Hirose, K., Lujaniene, G., Nakano, M., Plastino,W., Sykora, I., Bartok, J., Gazak, M., 2013. Dispersion of Fukushima radionuclides in the global atmosphere and the ocean. Appl. Radiat. Isot. 81, 383–392. https://doi.org/10.1016/j.apradiso.2013.03.058.

Pudykiewicz, J., 1988. Numerical simulation of the transport of radioactive cloud from the Chernobyl nuclear accident. Tellus B Chem. Phys. Meteorol. 40, 241-259. https://doi.org/10.1111/j.1600-0889.1988.tb00295.x.

Pullen, J., Chang, J., Hanna, S., 2013. Air-sea transport, dispersion, and fate modeling in the vicinity of the Fukushima nuclear power plant e a special conference session summary. Bull. Am. Meteorol. Soc. 94, 25-30. https://doi.org/10.1175/BAMS-D-11-00158.1.

Quérel, A, Roustan, Y., Quélo, D., Benoit, J.-P., 2015. Hints to discriminate the choice of wet deposition models applied to an accidental radioactive release. Int. J. Environ. Pollut. 56, 268-279. https://doi.org/10.1504/IJEP.2015.077457.

Retalis, D., Pitta, A., 1989. Effects on electrical parameters at Athens, Greece by radioactive fallout from a nuclear power plant accident. J. Geophys. Res.. 94, 13093–13097, https://doi.org/10.1029/JD094iD11p13093.

Retalis, D.A., 1987. Chernobyl Reactor Accident Consequences On Small Atmospheric Ions Concentration Above Athens. Pure Appl. Geophys. 125, 669-678. https://doi.org/10.1007/BF00879578.

Rycroft, M.J., Harrison, R.G., Nicoll, K.A., Mareev, E.A., 2008. An Overview of Earth's Global Electric Circuit and Atmospheric Conductivity. Space Sci. Rev. 137, 83. https://doi.org/10.1007/s11214-008-9368-6.

Rycroft, M.J., Nicoll, K.A., Aplin, K., Harrison, R.G., 2012. Recent advances in global electric circuit coupling between the space environment and the troposphere. J. Atmos. Sol-Terr. Phys. 90-91, 198-211. https://doi.org/10.1016/j.jastp.2012.03.015.

Sanada, Y., Matsunaga, T., Yanase, N., Nagao, S., Amano, H., Takada, H., Tkachenko, Y., 2002. Accumulation and potential dissolution of Chernobyl-derived radionuclides in river bottom sediment. Appl. Radiat. Isot. 56, 751-760. https://doi.org/10.1016/S0969-8043(01)00274-3.

Saito, K., Shimbori, T., Draxler, R., Hara, T., Toyoda, E., Honda, Y., Nagata, K., Fujita, T., Sakamoto, M., Kato, T., Kajino, M., Sekiyama, T.T., Tanaka, T.Y., Maki, T., Terada, H., Chino, M., Iwasaki, T., Hort M.C., Leadbetter, S.J., Wotawa, G., Arnold, D., Maurer, C., Malo, A., Servranckx, R., Chen, P., 2015. Contribution of JMA to the WMO Technical Task Team on Meteorological Analyses for Fukushima Daiichi Nuclear Power Plant Accident and Relevant Atmospheric Transport Modeling at MRI. Technical Reports of the Meteorological Research Institute, No. 76, Japan Meteorological Agency, DOI : 10.11483/mritechrepo.76.

Sato, Y., Takigawa, M., Sekiyama, T.T., Kajino, M., Terada, H., et al. 2018. Model Intercomparison of Atmospheric ^{137}Cs From the Fukushima Daiichi Nuclear Power Plant Accident: Simulations Based on Identical Input Data. J. Geophys. Res. Atmos. 123, 11, 748-11,765. https://doi.org/10.1029/2018JD029144.

SCJ (Science Council of Japan), 2014. A review of the model comparison of transportation and deposition of radioactive materials released to the environment as a result of the Tokyo Electric Power Company's Fukushima Daiichi Nuclear Power Plant accident, Committee on Comprehensive Synthetic Engineering, pp.103.

Shigeno, N., Takizawa, T., Itoh, N., Yokoyama, M., Owada, T., 2001. Preliminary test for atmospheric electricity measured using an electrostatic sensor, Gijutsu Hookoku, 112, 8-13.

Smith JN, Rossi V, Buesseler KO, Cullen JT, Cornett J, Nelson R, Macdonald, A. M.,Robert, M., Kellogg, J., 2017. Recent Transport History of Fukushima Radioactivity in the Northeast Pacific Ocean. Environmental Science & Technology; 51: 10494-10502. DOI: 10.1021/acs.est.7b02712

Stoehlker, U., Nikkinen, M., Gheddou, A., 2011. Detection of radionuclides emitted during the Fukushima nuclear accident with the CTBT radionuclide network, in: Proceedings of the 2011 Monitoring Research Review: Ground-Based Nuclear Explosion Monitoring, 715-724. https://www.osti.gov/biblio/1027453-proceedings-monitoring-research-review-ground-based-nuclear-explosion-monitoring-technologies.

Stohl, A., Seibert, P., Wotawa, G., Arnold, D., Burkhart, J.F., Eckhardt, S., Tapia, C., Vargas, A., Yasunari, T.J., 2012. Xenon-133 and caesium-137 releases into the atmosphere from the Fukushima Dai-ichi nuclear power plant: determination of the source term, atmospheric dispersion, and deposition. Atmos. Chem. Phys. 12, 2313-2343. https://doi.org/10.5194/acp-12-2313-2012.

Takeda, M., Yamauchi. M., Makino, M., Owada, T., 2011. Initial effect of the Fukushima accident on atmospheric electricity. Geophys. Res. Lett. 38, L15811, https://doi.org/10.1029/2011GL048511.

Talerko, N., 2005a. Mesoscale modelling of radioactive contamination formation in Ukraine caused by the Chernobyl accident. J. Environ. Radioact. 78, 311-329. https://doi.org/10.1016/j.jenvrad.2004.04.008.

Talerko, N., 2005b. Reconstruction of ^{131}I radioactive contamination in Ukraine caused by the Chernobyl accident using atmospheric transport modeling. J. Environ. Radioact. 84, 343-362. https://doi.org/10.1016/j.jenvrad.2005.04.005.

Terada, H., Chino, M., 2008a. Development of an atmospheric dispersion model for accidental discharge of radionuclides with the function of simultaneous prediction for multiple domains and its evaluation by application to the Chernobyl nuclear accident. J. Nucl. Sci. Technol. 45, 920–931. 10.1080/18811248.2008.9711493.

Terada, H., Katata, G., Chino, M., Nagai, H., 2012. Atmospheric discharge and dispersion of radionuclides during the Fukushima Dai-ichi Nuclear Power Plant accident. Part II: verification of the source term and analysis of regional-scale atmospheric dispersion. J. Environ. Radioact. 112, 141–154. https://doi.org/10.1016/j.jenvrad.2012.05.023.

Terada, H., Nagai, H., Furuno, A., Kakefuda, T., Harayama, T., Chino, M., 2008b. Development of worldwide version of system for prediction of environmental emergency dose information: WSPEEDI 2nd version. Trans. At. Energy Soc. Jpn. 7, 257–267, [in Japanese with English abstract]. https://doi.org/10.3327/taesj.J07.045.

Thakur, P., Ballard, S., Nelson, R., 2013. An overview of Fukushima radionuclides measured in the northern hemisphere. Sci. Total Environ. 458-460, 577-613. DOI:10.1016/j.scitotenv.2013.03.105.

Tsubono, T., Misumi, K., Tsumune, D., Bryan, F.O., Hirose, K., Aoyama, M., 2016. Evaluation of radioactive cesium impact from atmospheric deposition and direct release fluxes into the North Pacific from the Fukushima Daiichi nuclear power plant. Deep Sea Res. Part 1 Oceanogr. Res. Pap. 115, 10-21. https://doi.org/10.1016/j.dsr.2016.02.019.

Tsunume, D., Tsubono, T., Aoyama, M., Hirose, K., 2012. Distribution of oceanic ^{137}Cs from the Fukushima Dai-ichi Nuclear Power Plant simulated numerically by a regional ocean model. J. Environ. Radioact. 111, 100-08. https://doi.org/10.1016/j.jenvrad.2011.10.007.

Tuomi T.J., 1982. The atmospheric electrode effect over snow. J. Atmos. Sol. Terr. Phys. 44, 737-745. https://doi.org/10.1016/0021-9169(82)90002-2.

Tuomi T.J., 1989. Ten Year Summary 1977-1986 of Atmospheric Electricity Measured at Helsinki-Vantaa Airport, Finland. Geophysica 25, 1-20.

Tuomi, T.J., 1988. Observations of atmospheric electricity 1986. Geophys. Publ. 7, 551.506.1, Finish Meteorological Institute, Helsinki, 61 pp.

Uman, M.A., 1986. All about lightning, 173 pp, ISBN 0-486-25237-X, Dover Pub. Inc., Mineola, USA.

UNSCEAR (United Nations Scientific Committee on the Effect of Atomic Radiation), 2000. Report to the General Assembly with Scientific Annexes, Volume II, Annex J - Exposures and effects of the Chernobyl accident. UNSCEAR, United Nations, New York.

UNSCEAR (United Nations Scientific Committee on the Effect of Atomic Radiation), 2013. Report to the General Assembly with Scientific Annexes, Volume I, Annex A - Levels and effects of Radiation Exposure due to the nuclear accident after the 2011 great east - Japan earthquake and tsunami, UNSCEAR, United Nations, New York.

Warzecha, S., 1987. Results of atmospheric electricity measurements at Swider after the Chernobyl nuclear power plant accident. Publs. Inst. Geophys. Pol. Acad. Sc., D-26 (198).

Warzecha, S., 1991. Long-lasting radioactive contamination at Swider and its effect on the atmospheric electricity parameters after the Chernobyl nuclear power plant accident. Publs. Inst. Geophys. Pol. Acad. Sc., D-35 (238).

Williams, E., Mareev, E., 2014. Recent progress on the global electrical circuit. Atmos. Res. 135-136, 208-227. http://doi.org/10.1016/j.atmosres.2013.05.015.

Williams, E.R., 2009. The global electrical circuit: A review. Atmos. Res. 91, 140-152. http://doi.org/10.1016/j.atmosres.2008.05.018.

Winiarek, V., Bocquet, M., Saunier, O., Mathieu, A., 2012. Estimation of errors in the inverse modeling of accidental release of atmospheric pollutant: application to the reconstruction of the cesium-137 and iodine-131 source terms from the Fukushima Daiichi power plant. J. Geophys. Res. 117, D05122. https://doi.org/10.1029/2011JD016932.

WMO (World Meteorological Organization), 2013. The World Meteorological Organization's Evaluation of Meteorological Analyses for the Radionuclide Dispersion and Deposition from the Fukushima Daiichi Nuclear Power Plant Accident. Report on the third meeting of the WMO Task Team on meteorological analyses for the Fukushima-Daiichi nuclear power plant accident, annex III, http://www.wmo.int/pages/prog/www/CBS-Reports/documents/WMO_fnpp_final_AnnexIII_4Feb2013_REVISED_17June2013.pdf.

Yamauchi, M., 2012. Secondary wind transport of radioactive materials after the Fukushima accident. Earth Planets Space 64, e1-e4. https://doi.org/10.5047/eps.2012.01.002.

Yamauchi, M., Takeda, M., Makino, M., Owada, T., Miyagi, I., 2012. Settlement process of radioactive dust to the ground inferred by the atmospheric electric field measurement. Ann. Geophys. 30, 49-56. https://doi.org/10.5194/angeo-30-49-2012.

Yamauchi, M., Takeda, M., Nagamachi, S., 2018. Effect of enhanced ionizing radiation on the cloud electricity after the Fukushima nuclear accident. Earth Planets Space 70, 48. https://doi.org/10.1186/s40623-018-0780-1.

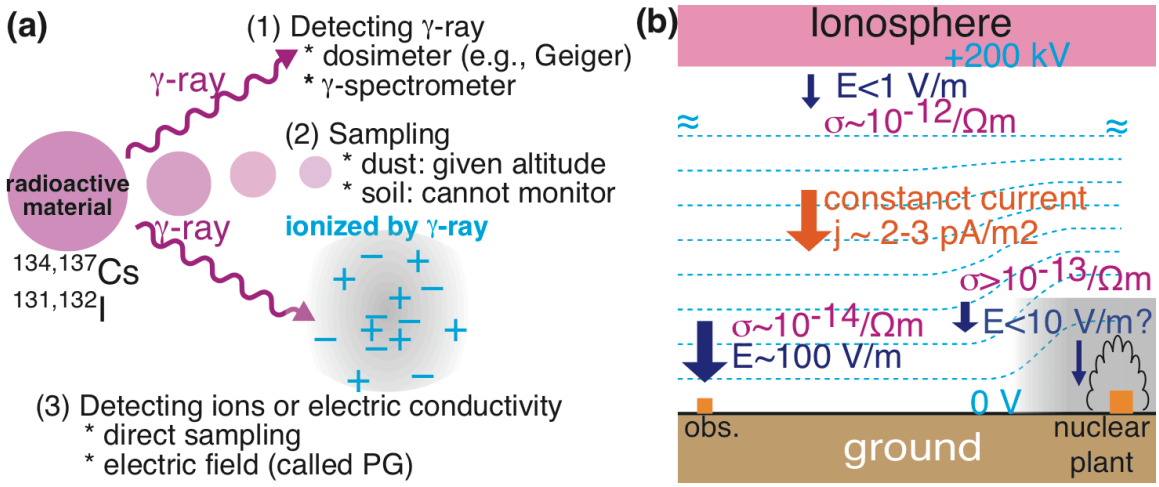

Figure 1. Illustrations of the monitoring principle of enhanced ionized radiation in the atmosphere: (a) Instead of direct detection of floating radioactive materials or ionizing radiation, one can also monitor the resultant ion density or even the vertical electric field (Potential Gradient: PG), (b) Local PG decreases (distance between equipotential surface increases) if the local ionospheric conductivity increases because the background electric field that is maintained on a global scale between the ionosphere and the ground. The PG works under fair weather when electric field due to free electric charges (such as electrified cloud) is not significant compared to background electric field.

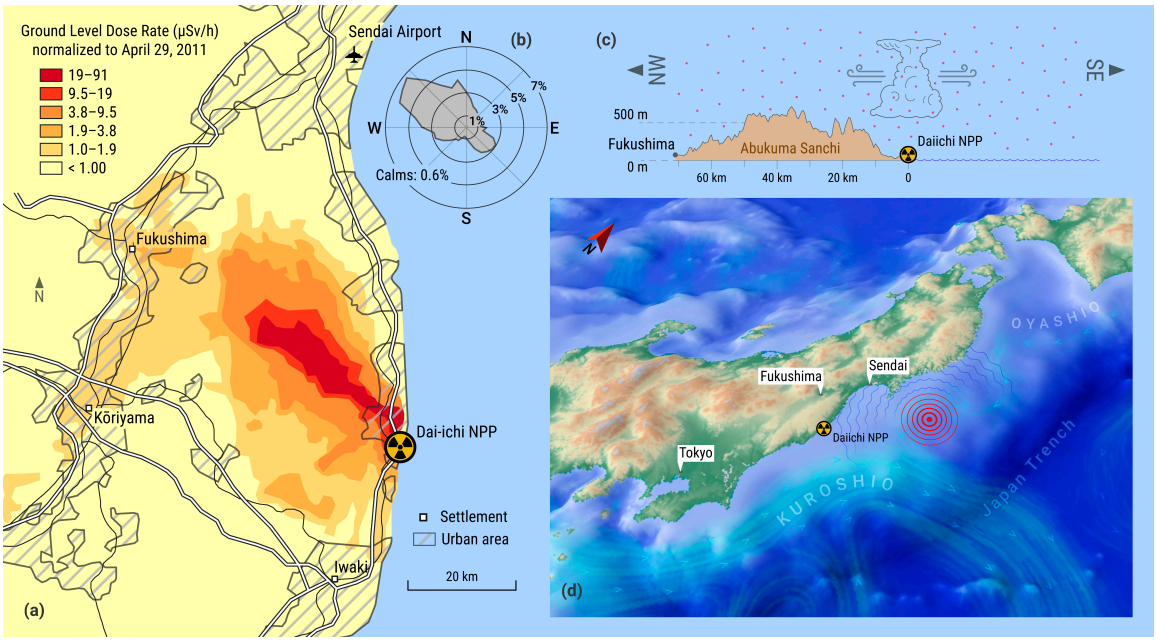

Figure 2. (a) Dose measurement map based on airborne monitoring map from April 6 to 29 by MEXT and DOE (Readings of air dose rate 1 m from the ground monitored inside 80 km zone of FNPP) (MEXT, 2011), (b) A wind rose of Sendai Airport (situated about 90 km from FNPP), the seven-year March summary (March 1, 2012 – March 31, 2018) (IEM), (c) The terrain profile between FNPP and the city of Fukushima with an Abukuma Sanchi Mountain situated between them and a schematic diagram of a dominant radionuclides release to the NW direction (to inland areas, toward the city of Fukushima) and the SE direction (to the ocean), (d) The 3D map showing topography and bathymetry near FNPP and epicenter of the earthquake. The center of concentric circles represents the epicenter of the earthquake which occurred near the Japan Trench, a line where the Pacific plate is subducting under the North American plate. Turquoise flow lines and arrows represent ocean currents.

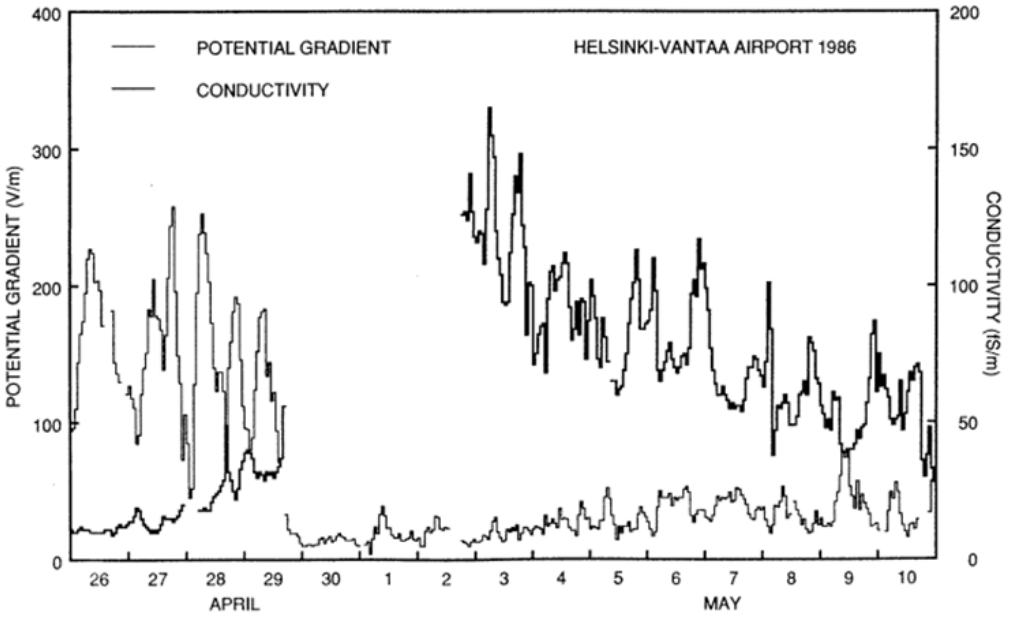

Figure 3. One-hour resolution PG (solid line) and atmospheric conductivity (bold line) at Helsinki for one month in April-May 1986, when the Chernobyl nuclear accident took place (after Tuomi, 1988). Rain-induced fallout took place on April 29, 1986.

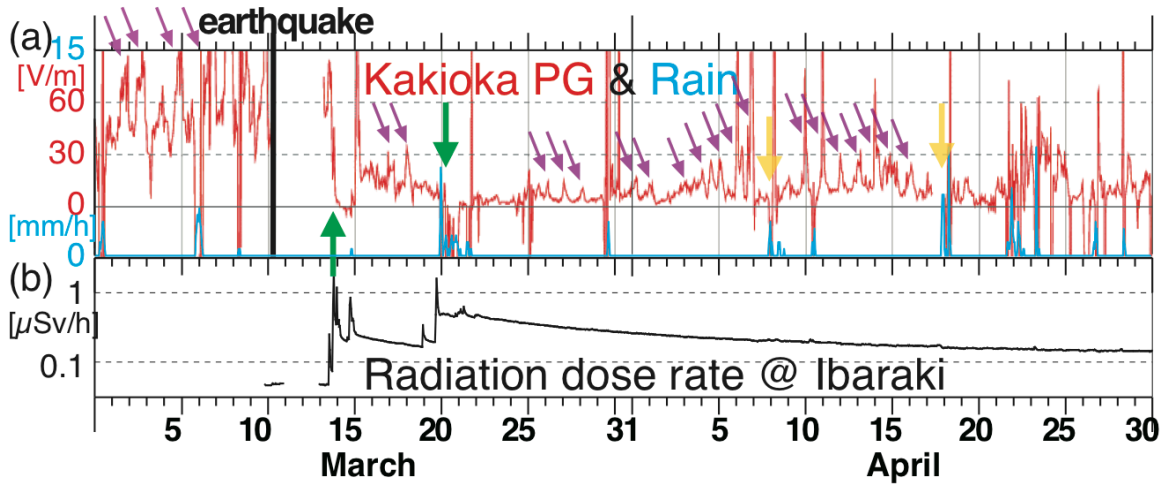

Figure 4. (a) Hourly averaged PG (red line) and one-hour accumulated rainfall (blue line) at Kakioka. (b) Hourly averaged radiation dose rate at Ibaraki-cho (nearest station of radiation observation to Kakioka). The time resolutions of raw data are 1 second for PG data and 10 minutes for the rainfall and radiation dose rate. The data gap from March 11 to ~March 14 is due to the power failure caused by the earthquake. The purple arrows in the upper panel indicate variation due to diurnal wind under fair weather, with peak local time (LT) near noon after the accident whereas it is 3-4 LT before the accident (Yamauchi et al., 2012).

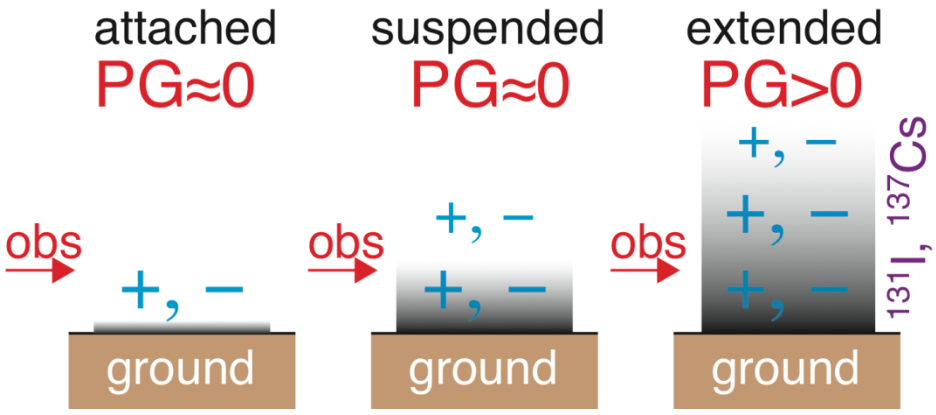

Figure 5. Expected PG for different degrees of contamination: firmly-attached (or migrated), loosely floating (or suspended near the ground), and re-suspended to extended altitude (Yamauchi et al., 2012).

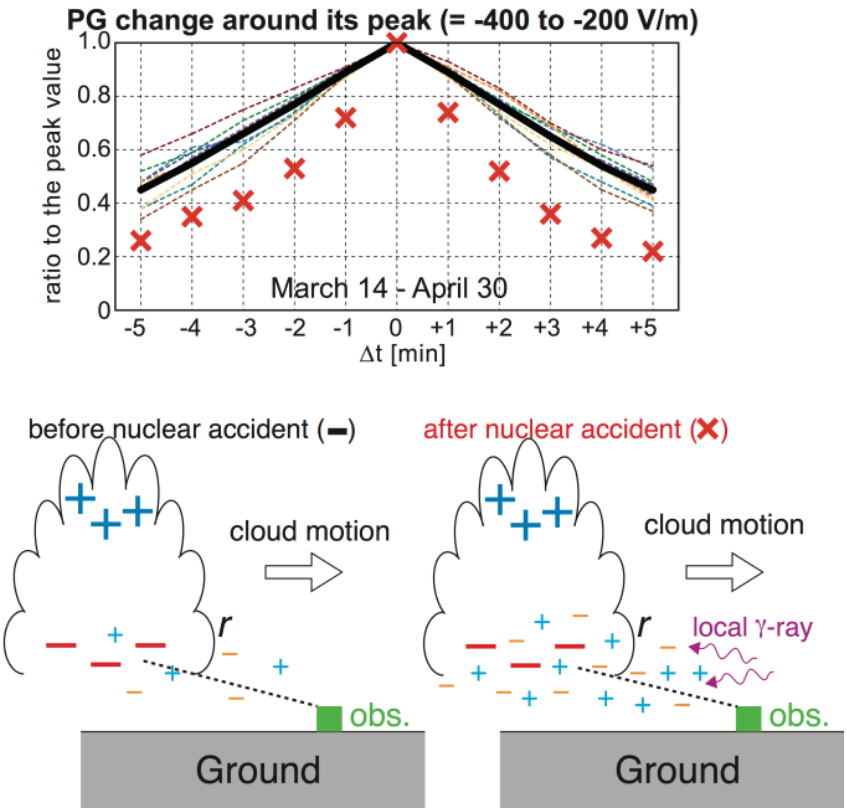

Figure 6. Relative PG values compared to peak values during 10 min centered at the peak time (top) and illustration of electrostatic shielding of cloud charge by surrounding ions (bottom) (Yamauchi et al., 2018). Red X marks are for 2011, dashed lines are for the other years, and the thick line is for the average. The shielding is larger for longer distances (with more shielding charges).